ETH
Eidgenössische Technische Hochschule Zürich
Swiss Federal Institute of Technology Zurich

Seminar for Applied Mathematics SAM

Electromagnetic Port Boundary Conditions: Topological and Variational Perspective

R. Hiptmair and J. Ostrowski

Research Report No. 2020-27
May 2020

Seminar für Angewandte Mathematik
Eidgenössische Technische Hochschule
CH-8092 Zürich
Switzerland

Submitted to Int. J. Numerical Modelling

Electromagnetic Port Boundary Conditions: Topological and Variational Perspective

R. Hiptmair* J. Ostrowski†

2020-05-05

Abstract

We present a comprehensive and variational approach to the coupling of electromagnetic field models with circuit-type models. That coupling relies on integral non-local quantities like voltage and current for electric ports, magnetomotive force and magnetic flux for magnetic ports, and linked currents and fluxes for "tunnels" in the field domain. These quantities are closely linked to non-bounding cycles studied in algebraic topology and they respect electromagnetic power balance laws. We obtain two dual variational formulations, called **E**-based and **H**-based, which provide a foundation for finite-element Galerkin discretization.

Keywords. field-circuit coupling, (M)ECE models, relative co-homology, electric and magnetic ports, finite elements

1 Introduction

A central issue in computional electromagnetics is the coupling of full field descriptions of electromagnetic phenomena used in one region of space ("field domain") with "lumped-element" circuit models (network models/graphical models) in another region of space ("circuit domain"). Both talk to each other through well-defined zones on the interface, known as ports. Details are given in Section 2.

In this article we present a comprehensive and *variational treatment* of this coupling based on the two ideas that have emerged as the underpinning of modern field-circuit coupling approaches:

(I) Electric and/or magnetic coupling between field and circuity domain is entirely channeled through the ports. We discuss the profound consequences in Section 3.1.

(II) The coupling through ports can completely be described by integral/non-local field quantities, see Section 5 for explanations.

In particular, this approach paves the way for introducing any kind of "lumped parameter excitations" into full Maxwell field models both in time and frequency domain. It permits us to imposed voltages, currents, and linked fluxes in the most general fashion.

Of course, also this work stands on the shoulders of giants, in particular on those of Alain Bossavit, whose 2000 seminal article on "Most general non-local boundary conditions for the Maxwell equations in a bounded region" [2] developed several key ideas

*SAM, ETH Zurich, CH-8092 Zurich, hiptmair@sam.math.ethz.ch

†ABB Switzerland Ltd., Corporate Research, Segelhofstr. 1, CH-5405 Baden

that also pervade this work. The most important is the insight that non-local coupling quantities are of *topological nature* and closely connected to profound mathematical concepts investigated in (co-)homology theory a field of algebraic topology. We will explain this in Section 3.2. It is a pity that, probably owing to "inscrutable mathematics", A. Bossavit's topology-centered perspective has not received due attention. An exception is the work by L. Kettunen and S. Suuriniemi [17, 18]. What their work has in common with ours is the appreciation of the role of the fine structure of homology spaces, see Section 3.2.

Another fundamental idea from [2] is the connection between topological (Poincaré) duality and integration by parts, which we will discuss in Section 4. As a consequence, energy/power balance laws naturally emerge, commensurate with their central role in field-circuit coupling, highlighted, for instance, in [1] and [11].

We also point out that the above coupling "axioms" (II) and (I) have also been proposed by G. Ciuprina, D. Ioan and co-workes to lay the foundations of the so-called (M)ECE-technique for defining and classifying port conditions, see [4, 13] and [5, Sect. 5.2.1]. These works, extending the final paragraph of [2], also link non-local boundary conditions with discretizations of Maxwell's equations. We will address this in Section 6.

Our main contribution consists in the synthesis of all these ideas and their elaboration in a *function-space variational framework*, leading to the all-encompassing variational equations (37, "**E**-based") and (40, "**H**-based"), which serve as a natural starting point for Galerkin discretization. We deliberately opted for a rather mathematical treatment and hope that we have kept the right balance of intuitive and rigorous arguments. In any case, in the final Section 7 we discuss a very concrete circuit-field coupling problem in frequency domain, in order to demonstrate how to extract a relevant **E**-based finite-element model employing our general ideas.

2 Geometric Setting

We consider the linear Maxwell's equations governing the evolution of electromagnetic fields on a *bounded Lipschitz domain* $\Omega \subset \mathbb{R}^3$, which we call the "field domain". As in the introduction of [2], it is coupled to the rest of the universe through its boundary $\Gamma := \partial\Omega$, which is *partitioned* into four different parts:

$$\overline{\Gamma} = \overline{\Gamma}_E \cup \overline{\Gamma}_M \cup \overline{\Gamma}_I \cup \overline{\Gamma}_R \,,$$

with mutually disjoint interior and piecewise smooth boundaries. They are meant to designate:

- Γ_E is the area occupied by **E**lectric contacts,
- Γ_M stands for **M**agnetic contacts,
- Γ_I is an **I**nsulated part of the boundary,
- and Γ_R is an artificial boundary on which **R**adiation conditions are to be imposed.

The contact boundaries have to be topologically simple in the sense of the following assumption.

Assumption 1. *(i) Both Γ_E and Γ_M are the union of* topologically trivial *ports*

$$\Gamma_E = \Gamma_E^1 \cup \cdots \cup \Gamma_E^{N_E} \quad , \quad \Gamma_M = \Gamma_M^1 \cup \cdots \cup \Gamma_M^{N_M} \,, \quad N_E, N_M \in \mathbb{N}_0 \,,$$

all of which have a positive distance from each other.

(ii) The radiation boundary is strictly separated from the other parts of Γ.

Here, topogically trivial means that the ports are simply connected (homeomorphic to a disk). The reader can imagine them as images of disks under bi-Lipschitz mappings.

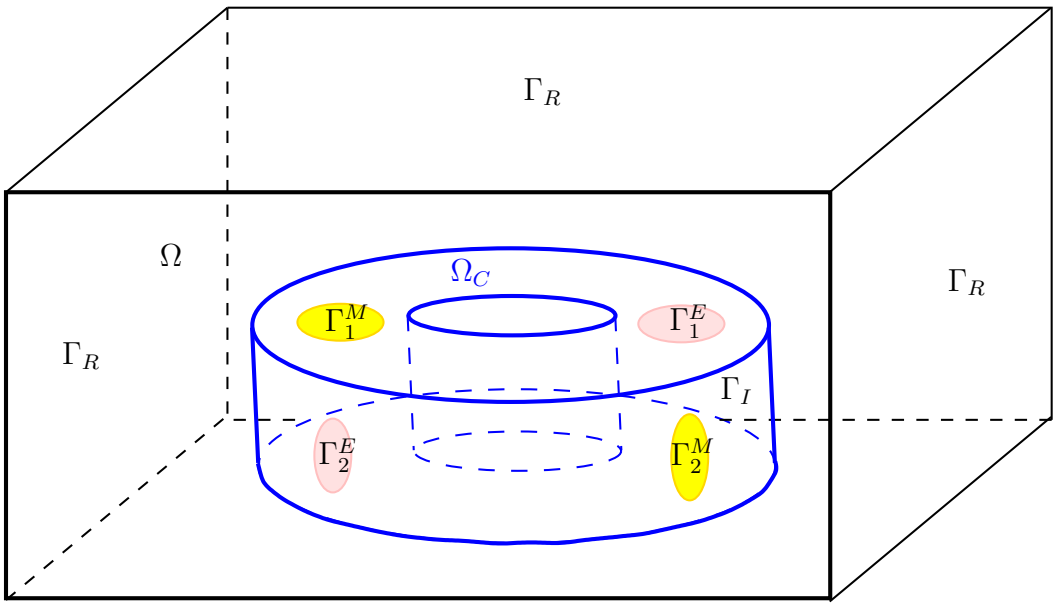

Figure 1: A typical situation compliant with Assumption 1 ($N_E = N_M = 2$): radiation conditions are imposed on the surface Γ_R of the artificial computational domain Ω (black box), the other boundary parts couple to the "circuit domain" Ω_C (blue hollow cylinder).

A typical situation is sketched in Fig. 1. Complicated electric circuits occupy a region of space, the "circuit domain" Ω_C, which is tiny compared to the characteristic electromagnetic wavelength. They interact with the electromagnetic fields outside, where wave propagation cannot be neglected. The unbounded domain $\mathbb{R}^3 \setminus \overline{\Omega_C}$ is truncated to Ω and the impact of truncation is taken into account by absorbing boundary conditions on Γ_R.

Of course, the situation could be reversed with Ω a bounded cavity in Ω_C, see Fig. 2. This can be appropriate when using the full Maxwell's equations locally in order to take into account both capacitive and inductive effects, though wave propagation may not be important. In Section 7 we will document a numerical simulation in such a setting.

For the bulk of our considerations the truncation by Γ_R does not matter much, and, thus, in large parts of the remainder of this article we just ignore the radiation boundary: We assume $\Gamma_R = \emptyset$. In addition, for the sake of simplicity we deal with connected circuit domains only, which implies that $\Gamma = \overline{\Gamma}_E \cup \overline{\Gamma}_M \cup \overline{\Gamma}_I = \partial\Omega_C$ is connected, too.

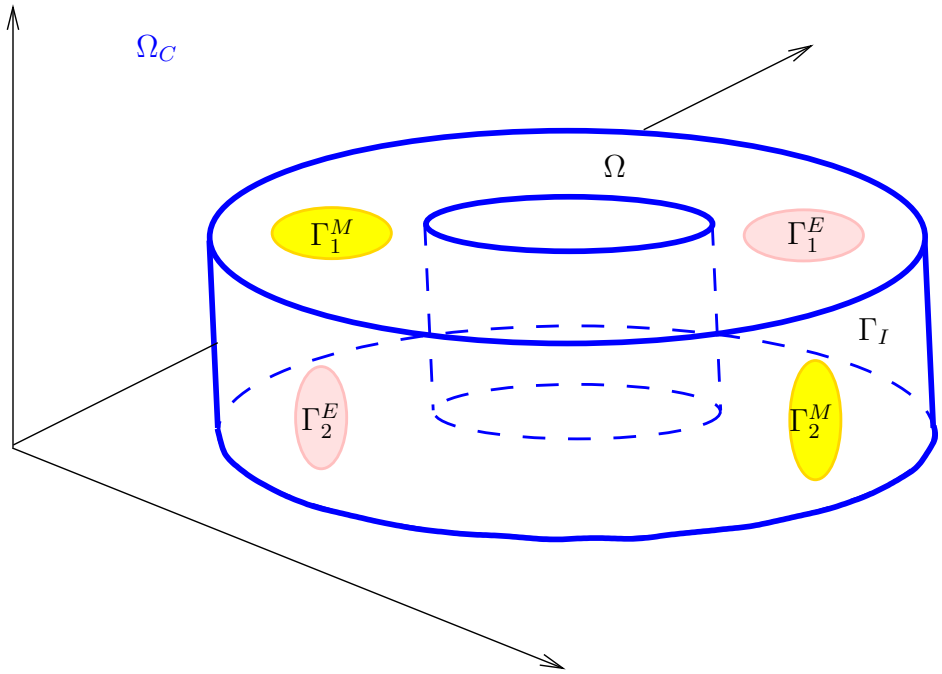

Figure 2: Another situation covered by Assumption 1 ($N_E = N_M = 2$): The circuit domain Ω_C is the unbounded complement of the bounded field domain Ω_C, here represented by the blue hollow cylinder.

3 Boundary Conditions

3.1 Function Spaces for Electromagnetic Fields

Recall that the space of finite-energy electric and magnetic fields in Ω is the Sobolev space[1]

$$\boldsymbol{H}(\mathbf{curl},\Omega) := \{\mathbf{v} \in \boldsymbol{L}^2(\Omega) : \ \mathbf{curl}\,\mathbf{v} \in \boldsymbol{L}^2(\Omega)\} \ .$$

To take into account the ports in a variational setting, we rely on two special closed subspaces. Their definition involves the two tangential traces

$$\boldsymbol{\gamma_t}\mathbf{u}(\boldsymbol{x}) := \boldsymbol{n}(\boldsymbol{x}) \times (\mathbf{u}(\boldsymbol{x}) \times \boldsymbol{n}(\boldsymbol{x})) \quad , \quad \boldsymbol{\gamma}_\times\mathbf{u}(\boldsymbol{x}) := \mathbf{u}(\boldsymbol{x}) \times \boldsymbol{n}(\boldsymbol{x}) \ , \quad \boldsymbol{x} \in \Gamma \ ,$$

first defined for smooth vectorfields and then extended to continuous surjective mappings $\boldsymbol{\gamma_t} : \boldsymbol{H}(\mathbf{curl},\Omega) \to \boldsymbol{H}^{-\frac{1}{2}}(\mathrm{curl}_\Gamma,\Gamma)$ and $\boldsymbol{\gamma}_\times : \boldsymbol{H}(\mathbf{curl},\Omega) \to \boldsymbol{H}^{-\frac{1}{2}}(\mathrm{div}_\Gamma,\Gamma)$, respectively [3, Thm. 1]. Note that products of these two traces yield "Poynting vectors", that is power-flux two-forms: $\boldsymbol{\gamma_t}\mathbf{E}\cdot\boldsymbol{\gamma}_\times\mathbf{H} = (\mathbf{E}\times\mathbf{H})\cdot\boldsymbol{n}|_\Gamma$. This is closely related to the integration by parts formula

$$\int_\Omega \mathbf{U}\cdot\mathbf{curl}\,\mathbf{V} - \mathbf{curl}\,\mathbf{U}\cdot\mathbf{V}\,\mathrm{d}\boldsymbol{x} = \int_{\partial\Omega} \boldsymbol{\gamma}_\times\mathbf{U}\cdot\boldsymbol{\gamma_t}\mathbf{V}\,\mathrm{d}S \quad \forall \mathbf{U},\mathbf{V} \in \boldsymbol{H}(\mathbf{curl},\Omega) \ , \tag{1}$$

and the fact that the trace spaces $\boldsymbol{H}^{-\frac{1}{2}}(\mathrm{curl}_\Gamma,\Gamma)$ and $\boldsymbol{H}^{-\frac{1}{2}}(\mathrm{div}_\Gamma,\Gamma)$ are in duality with respect to the $\boldsymbol{L}^2(\Gamma)$-inner product [3, Thm. 2].

Now we can introduce the key function spaces

- for electric fields (space "E" in [2])

$$\mathcal{V}_E := \{\mathbf{E} \in \boldsymbol{H}(\mathbf{curl},\Omega) : \ \boldsymbol{\gamma_t}\mathbf{E} = 0 \text{ on } \Gamma_E \ , \ \mathrm{curl}_\Gamma\,\boldsymbol{\gamma_t}\mathbf{E} = 0 \text{ on } \Gamma_I\} \ , \tag{2}$$

[1] Concerning function spaces we adhere to notational conventions widely adopted in the mathematical analysis of numerical methods in computational electromagnetism, see [16, Ch. 3] and also [3, Sect. 2] for more exotic trace spaces.

- and for the magnetic field (space "ℍ" in [2])

$$\mathcal{V}_M := \{\mathbf{H} \in \boldsymbol{H}(\mathbf{curl}, \Omega) : \boldsymbol{\gamma}_\times \mathbf{H} = 0 \text{ on } \Gamma_M\,,\ \mathrm{div}_\Gamma \boldsymbol{\gamma}_\times \mathbf{H} = 0 \text{ on } \Gamma_I\}\,, \quad (3)$$

Recall that the scalar-valued surface differential operators curl_Γ and div_Γ for tangential traces are defined as

$$\mathrm{curl}_\Gamma(\boldsymbol{\gamma_t}\mathbf{V}) = \mathrm{div}_\Gamma(\boldsymbol{\gamma}_\times \mathbf{V}) = \gamma_{\boldsymbol{n}}(\mathbf{curl}\,\mathbf{V}) \quad \text{for} \quad \mathbf{V} \in \boldsymbol{H}(\mathbf{curl}, \Omega)\,, \quad (4)$$

$\gamma_{\boldsymbol{n}}$ the normal components trace, which immediately gives them a meaning for tangential vectorfields in the trace spaces $\boldsymbol{H}^{-\frac{1}{2}}(\mathrm{curl}_\Gamma, \Gamma)$ and $\boldsymbol{H}^{-\frac{1}{2}}(\mathrm{div}_\Gamma, \Gamma)$, respectively, as hinted by the notations.

What motivates the choice of the spaces $\mathcal{V}_E$ and $\mathcal{V}_M$? As for an electric contact $\Gamma_E^\ell \subset \Gamma_E$ you may think of a perfect conductor being attached to Ω, from which any electric field is expelled: $\boldsymbol{\gamma_t}\mathbf{E}|_{\Gamma_E} = 0$ for the electric field $\mathbf{E} \in \boldsymbol{H}(\mathbf{curl}, \Omega)$. Similarly, the magnetic field is blocked at the magnetic contact zone: $\boldsymbol{\gamma}_\times \mathbf{H}|_{\Gamma_M} = 0$. Conversely, the insulating interface Γ_I cannot be penetrated by any fluxes, neither magnetic nor electric, which, in light of (4), is enforced by the boundary conditions built into the definitions (2) and (3) of $\mathcal{V}_E$ and $\mathcal{V}_M$.

Remark 2. At the radiation boundary we assume general linear impedance boundary conditions

$$\boldsymbol{\gamma_t}\mathbf{E} = \mathsf{Z}(\boldsymbol{\gamma}_\times \mathbf{H}) \quad \text{on} \quad \Gamma_R\,, \quad (5)$$

where Z is a suitable invertible linear operator, possibly *non-local both in space and time*, meant to offset the effect of truncation approximately. Therefore, (5) is often called an absorbing boundary condition. Note that the boundary conditions at Γ_R do not show up neither in the space $\mathcal{V}_E$ nor in $\mathcal{V}_M$.

3.2 Tool: (Co-)Homolgy

Co-homology and its dual theory, homology, is key to understanding obstructions to the existence of potential representations for functions in the kernel of differential operators, that is, obstructions to being in the range of other differential operators. This issue arises here, because both (2) and (3) define $\mathcal{V}_E$ and $\mathcal{V}_M$ as kernels of the surface differential operators curl_Γ and div_Γ, respectively.

(Co-)homology centers around the concepts of "cycle" and "boundary". We give an intuitive and geometric description, which, nevertheless captures their essence. A slightly more formal treatment from the perspective of chain calculus is offered in the introduction of [2].

Consider a non-degenerate[2] subset $\Sigma \subset \Gamma$ with sufficiently regular boundary. In addition, let σ denote a non-degenerate part of the boundary $\partial\Sigma$.

Definition 3 (Cycle)**.** A σ-relative *cycle* $\gamma \subset \Sigma$ is a directed curve, which is either a loop (closed curve) or is open and has both its endpoints located on σ.

Definition 4 (Bounding)**.** A σ-relative cycle γ is *bounding*, if there is a non-degenerate area $S \subset \Sigma$ such that $\gamma = \partial S \setminus \sigma$.

[2]Non-degenerate means that the closure of the interior of Σ in Γ must coincide with $\overline{\Sigma}$.

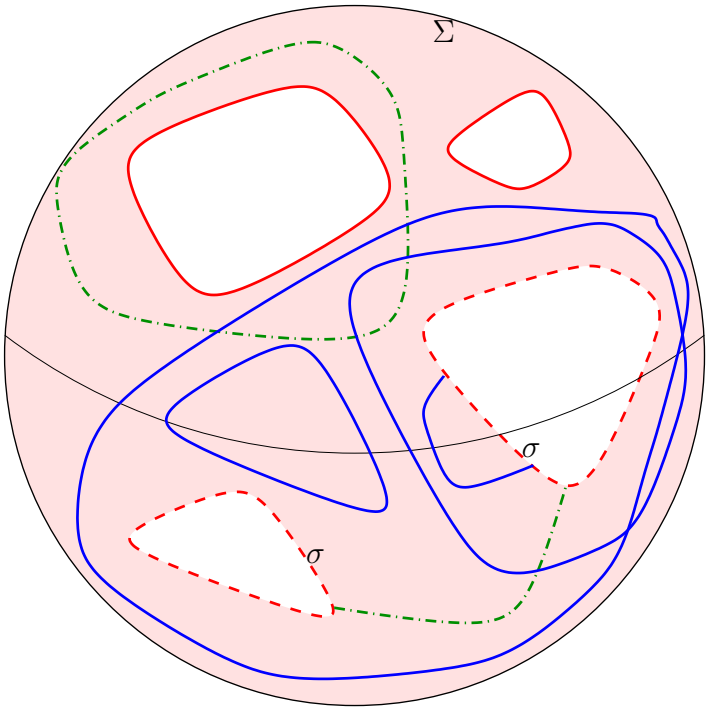

Figure 3: Γ is the surface of a sphere, Σ the pink area, the dashed - - - sections of its boundary constitute σ. The blue and green curves are σ-relative *cycles* in Σ. The blue cycles are *bounding*, the green are *not bounding*, both relative to σ.

Examples of bounding and non-bounding cycles are visualized in Fig. 3 taking the cue from [2, Fig. 1]. The following is a rephrasing of a fundamental result of (relative) co-homology theory for 2-surfaces concerning potential representations for the space of tangential vectorfields

$$\mathcal{W} := \left\{ \mathbf{v} \in \boldsymbol{H}(\mathrm{curl}_\Gamma, \Sigma) : \begin{array}{l} \mathrm{curl}_\Gamma \mathbf{v} = 0 \text{ in } \Sigma \,, \\ \mathbf{v} \text{ has vanishing tangential components on } \sigma \end{array} \right\} \tag{6}$$

based on the space of scalar functions

$$\mathcal{S} := \{ \varphi \in H^1(\Sigma) : \ \varphi|_\sigma = 0 \} \,. \tag{7}$$

Theorem 5. *There is a number $N \in \mathbb{N}_0$ and a finite set of*

(i) non-bounding (relative to σ) fundamental σ-relative cycles $\gamma_1, \ldots, \gamma_N$,

(ii) tangential co-homology vectorfields $\mathbf{c}_1, \ldots, \mathbf{c}_N \in \mathcal{W}$ satisfying

$$\int_{\gamma_j} \mathbf{c}_m \cdot \mathrm{d}s = \begin{cases} 1 & \text{for } m = j \,, \\ 0 & \text{else,} \end{cases} \qquad j, m \in \{1, \ldots, N\} \,, \tag{8}$$

such that, with $\mathcal{W}$ and $\mathcal{S}$ as in (6) *and* (7),

$$\mathcal{W} := \mathbf{grad}_\Gamma \mathcal{S} + \mathrm{span}\{\mathbf{c}_1, \ldots, \mathbf{c}_N\} \,. \tag{9}$$

Remark 6. The "$\frac{\pi}{2}$-rotated setting": If curl_Γ in (6) is replaced with div_Γ, then $\mathbf{curl}_\Gamma$ should substitute $\mathbf{grad}_\Gamma$ in (9).

Remark 7. We point out that Theorem 5 remains valid when replacing $\boldsymbol{H}(\mathrm{curl}_\Gamma, \Sigma)$ with $\boldsymbol{H}^{-\frac{1}{2}}(\mathrm{curl}_\Gamma, \Sigma)$ in (6) and $H^1(\Sigma)$ with $H^{\frac{1}{2}}(\Sigma)$ in (7), though zero boundary conditions on σ have to be rephrased as the existence of a zero extension in this case.

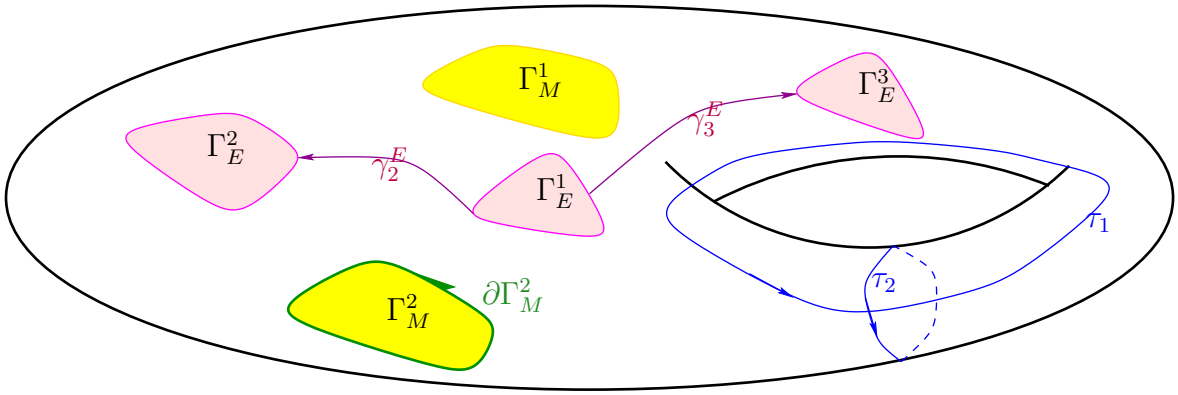

Figure 4: Torus-shaped Ω_C ($N_T = 2$); $N_E = 3$ electric ports in pink, $N_M = 2$ magnetic ports in yellow, fundamental cycles for the relative homology space $H_1(\Gamma_I, \partial\Gamma_E)$ are the "topological cycles" τ_1, τ_2 of class (T) in blue, the "electric connector cycles" γ_2^E, γ_3^E of class (CE) in purple, and the "magnetic port cycles" $\partial\Gamma_M^2$ of class (PE) in green.

Remark 8. In homology theory the cycles $\gamma_1, \ldots, \gamma_N$ mentioned in Theorem 5 are introduced as 1-chains that form a basis of the relative homology space $H_1(\Sigma, \sigma)$. From this perspective, the vector fields $\mathbf{c}_1, \ldots, \mathbf{c}_N$ should be regarded as 2D Euclidean 1-form vector proxies of representatives of a basis of the relative co-homology space $H^1(\Sigma, \sigma)$, [12, Sect. 2 & 5].

Let us return to the geometric setting outlined in the introduction and to the space $\mathcal{V}_E$ from (2). Using the notation established above, as regards the application of Theorem 5 to $\mathcal{V}_E$ we face the situation $\Sigma = \Gamma_I$ and $\sigma = \partial\Gamma_E$. We need a precise characterization of the σ-relative cycles γ_i. As has already been realized in [18, Sect. III.C], the fundamental cycles non-bounding relative to $\partial\Gamma_E$ fall into three different classes, see Fig. 4 (also for the color code):

(T) Fundamental non-bounding cycles ("topological cycles")

$$\tau_1, \ldots, \tau_{N_T} , \quad N_T := 2\beta_1(\Omega_C) ,$$

of Γ, where $\beta_1(\Omega_C)$ is the first Betti number of Ω_C, that is, the number of handles/tunnels of both the circuit domain Ω_C and the field domain Ω.

(CE) $N_E - 1$ directed curves $\gamma_2^E, \ldots, \gamma_{N_E}^E \subset \Gamma_I$ connecting Γ_E^1 with the other electric ports $\Gamma_E^2, \ldots, \Gamma_E^{N_E}$ ("electric connector cycles"),

(PE) the $N_M - 1$ oriented boundaries $\partial\Gamma_M^\ell$, $\ell = 2, \ldots, N_M$, of the magnetic ports $\Gamma_M^2, \ldots, \Gamma_M^{N_M}$ ("magnetic port cycles").

Hence, the number of Γ_E-relative fundamental cycles is

$$N := N_T + \max\{N_M, 1\} + \max\{N_E, 1\} - 2 , \tag{10}$$

and, by Theorem 5, it takes that many co-homology tangential vectorfields to fill the gap between $\mathcal{V}_E$ and gradients of functions that vanish on $\partial\Gamma_E$.

The considerations for $\mathcal{V}_M$ invoke Γ_M-relative homology. Again, three different classes of Γ_M-relative fundamental cycles can be identified in addition to class (T) from above, see Fig. 5:

(CM) $N_M - 1$ directed curves $\gamma_2^M, \ldots, \gamma_{N_M}^M$ from Γ_M^1 to every other magnetic port ("magnetic connector cycles"),

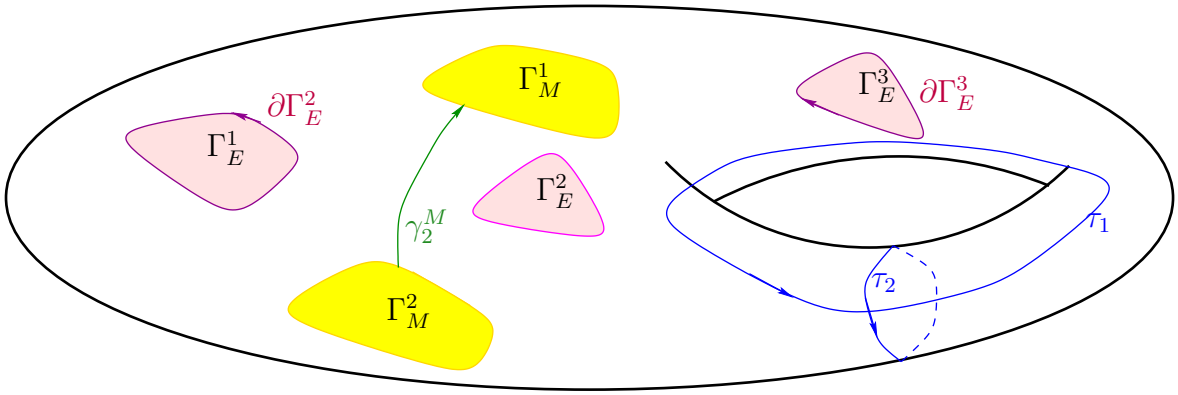

Figure 5: Torus-shaped Γ ($\beta_1(\Omega_C) = 1$); electric ports in pink, magnetic ports in yellow, Γ_M-relative fundamental cycles in Γ_I are τ_1, τ_2 of class (T) colored blue, γ_2^M of class (CM) in green, $\partial\Gamma_E^2, \partial\Gamma_E^3$ of class (PM) in purple.

(PM) the $N_E - 1$ boundaries $\partial\Gamma_E^k$, $k = 2, \ldots, N_E$, of the electric ports $\Gamma_E^2, \ldots, \Gamma_E^{N_E}$ ("electric port cycles").

Since $\partial\Gamma_I = \partial\Gamma_E \cup \partial\Gamma_M$, Poincaré-Lefschetz duality of homology theory guarantees that the Γ_E-relative fundamental cycles for $\mathcal{V}_E$ can be put in *duality* with the Γ_M-relative fundamental cycles for $\mathcal{V}_M$. This means that we can find finite sets of fundamental cycles of equal cardinality for both spaces and a bijective "pairing" between both sets that

- pairs the "topological" cycles of class (T) among themselves; these N_T cycles naturally come in pairs of dual cycles[3], *cf.* Assumption 12.
- pairs "connector cycles" of one set with "port cycles" of the other. Note that their numbers $N_E - 1$ and $N_M - 1$, respectively, agree.

Fig. 6 and [2, Fig. 2] illustrate this relationship. The paired cycles can always be chosen to intersect transversally; they will be called *dual* to each other and the unique dual cycle of a given cycle will be tagged with $\widehat{\ }$. Then above statements can be expressed formally as

$$\widehat{\tau_m} = \tau_{N_T-m+1} \quad \Leftrightarrow \quad \tau_m = \widehat{\tau_{N_T-m+1}}\,, \qquad m = 1, \ldots, N_T\,, \tag{11a}$$

$$\widehat{\gamma_k^E} = \partial\Gamma_E^k \quad \Leftrightarrow \quad \gamma_k^E = \widehat{\partial\Gamma_E^k}\,, \qquad k = 2, \ldots, N_E\,, \tag{11b}$$

$$\widehat{\gamma_\ell^M} = \partial\Gamma_M^\ell \quad \Leftrightarrow \quad \gamma_\ell^M = \widehat{\partial\Gamma_M^\ell}\,, \qquad \ell = 2, \ldots, N_M\,. \tag{11c}$$

3.3 Boundary scalar potentials

As we have seen in Theorem 5, tangential surface fields with vanishing $\mathbf{curl}_\Gamma/\mathrm{div}_\Gamma$ can be represented through surface scalar potentials plus contributions from low-dimensional co-homology spaces. First we focus on $\boldsymbol{\gamma_t}\mathcal{V}_E$ and the co-homology vectorfields associated with $\partial\Gamma_E$-relative non-bounding "electric connector cycles" of class (CE). Those co-homology vectorfields have a simple representation:

Let γ_k^E be a $\partial\Gamma_E$-relative fundamental cycle of class (CE) connecting Γ_E^1 and Γ_E^k, $k = 2, \ldots, N_E$. Then the associated tangential co-homology vectorfield $\mathbf{c} \in \mathcal{V}_E$ is given

[3] On a formal level the duality of (oriented) topological cycles can be expressed through their intersection numbers, see see [7, Sect. 6.4] and, in particular, Chapter 5 of [8].

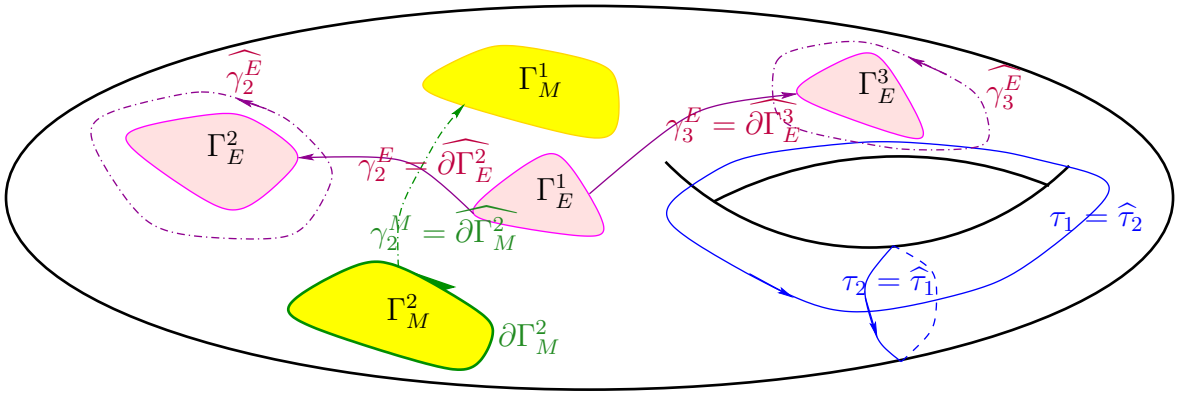

Figure 6: Torus-shaped Γ ($N_T = 2$, $N_E = 3$, $N_M = 2$): Γ_E-relative fundamental cycles for $\mathcal{V}_E$ as in Fig. 4 are drawn with solid lines, their *dual* Γ_M-relative fundamental cycles are drawn with dashed lines and are marked with a $\widehat{\ }$.

by

$$\mathbf{c} := \mathbf{grad}_\Gamma \varphi_E^k \quad \text{with} \quad \varphi_E^k \in H^1(\Gamma)\,, \quad \varphi_E^k\big|_{\Gamma_E^k} \equiv 1\,, \quad \varphi_E^k\big|_{(\Gamma_E \cup \Gamma_M)\setminus\Gamma_E^k} \equiv 0\,. \tag{12}$$

That $\mathbf{c}$ satisfies condition (8), $\int_{\gamma_n^E} \mathbf{c}\cdot\mathrm{d}s = \begin{cases} 1 & \text{for } n = k\,, \\ 0 & \text{else} \end{cases}$, is an immediate consequence of the fundamental theorem of calculus and the fact that the cycle γ_k^E connects the two electric ports Γ_E^k and Γ_E^1 with $\varphi_E^k\big|_{\Gamma_E^1} \equiv 0$. Moreover, let us write

- $\mathbf{c}_2^E, \ldots, \mathbf{c}_{N_M}^E \in \boldsymbol{H}(\mathrm{curl}_\Gamma, \Gamma) \cap \mathcal{V}_E$ for the $N_M - 1$ tangential co-homology vector-fields belonging to the Γ_E-relative non-bounding "magnetic port cycles" $\partial\Gamma_M^\ell$, $\ell = 2, \ldots, N_M$, in Γ_I of class (PE),
- and $\mathbf{t}_1^E, \ldots, \mathbf{t}_{N_T}^E \in \boldsymbol{H}(\mathrm{curl}_\Gamma, \Gamma) \cap \mathcal{V}_E$ for the tangential co-homology vectorfields corresponding to the "topological" Γ_E-relative non-bounding cycles $\tau_1, \ldots, \tau_{N_T}$ in Γ_I of class (T). As will become clear in Section 3.4, those can be chosen to vanish on $\Gamma_M \cup \Gamma_E$.

These co-homology vectorfields will be examined more closely in Section 3.4. Now we are in a position to characterize the tangential trace space of $\mathcal{V}_E$ as

$$\begin{aligned} \boldsymbol{\gamma_t}\mathcal{V}_E &= \{\mathbf{m} \in \boldsymbol{H}^{-\frac{1}{2}}(\mathrm{curl}_\Gamma, \Gamma) : \ \mathbf{curl}_\Gamma \mathbf{m} = 0 \text{ on } \Gamma_I,\ \mathbf{m} = 0 \text{ on } \Gamma_E\} \\ &= \mathbf{grad}_\Gamma \mathcal{S}_E + \sum_{\ell=2}^{N_M} \mathrm{span}\{\mathbf{c}_\ell^E\} + \sum_{m=1}^{N_T} \mathrm{span}\{\mathbf{t}_m^E\} + \widetilde{\boldsymbol{H}}^{-\frac{1}{2}}(\mathrm{curl}_\Gamma, \Gamma_M)\,, \end{aligned} \tag{13}$$

with the space of scalar potentials

$$\mathcal{S}_E := \widetilde{H}^{\frac{1}{2}}_{\Gamma_E}(\Gamma) + \sum_{k=2}^{N_E} \mathrm{span}\{\varphi_E^k\}\,, \quad \widetilde{H}^{\frac{1}{2}}_{\Gamma_E}(\Gamma) := \{\psi \in H^{\frac{1}{2}}(\partial\Omega) : \ \psi|_{\Gamma_E} = 0\}\,, \tag{14}$$

and $\widetilde{\boldsymbol{H}}^{-\frac{1}{2}}(\mathrm{curl}_\Gamma, \Gamma_M)$ standing for the space of tangential traces supported in $\overline{\Gamma}_M$:

$$\widetilde{\boldsymbol{H}}^{-\frac{1}{2}}(\mathrm{curl}_\Gamma, \Gamma_M) := \{\mathbf{v} \in \boldsymbol{H}^{-\frac{1}{2}}(\mathrm{curl}_\Gamma, \Gamma) : \ \mathrm{supp}\,\mathbf{v} \subset \overline{\Gamma}_M\}\,. \tag{15}$$

An analogous representation holds for the magnetic space $\mathcal{V}_M$:

$$\begin{aligned} \boldsymbol{\gamma}_\times \mathcal{V}_M &= \{\mathbf{j} \in \boldsymbol{H}^{-\frac{1}{2}}(\mathrm{div}_\Gamma, \Gamma) : \ \mathrm{div}_\Gamma \mathbf{j} = 0 \text{ on } \Gamma_S,\ \mathbf{j} = 0 \text{ on } \Gamma_M\} \\ &= \mathbf{curl}_\Gamma \mathcal{S}_M + \sum_{k=2}^{N_E} \mathrm{span}\{\mathbf{c}_k^M\} + \sum_{m=1}^{N_T} \mathrm{span}\{\mathbf{t}_m^M\} + \widetilde{\boldsymbol{H}}^{-\frac{1}{2}}(\mathrm{div}_\Gamma, \Gamma_E)\,, \end{aligned} \tag{16}$$

with the scalar potential space given by

$$\mathcal{S}_M := \widetilde{H}^{\frac{1}{2}}_{\Gamma_M}(\Gamma) + \sum_{\ell=2}^{N_M} \operatorname{span}\{\varphi_M^\ell\} \ , \quad \widetilde{H}^{\frac{1}{2}}_{\Gamma_M}(\Gamma) := \{\psi \in H^{\frac{1}{2}}(\partial\Omega) : \ \psi|_{\Gamma_M} = 0\} \ , \tag{17}$$

and a space $\widetilde{\boldsymbol{H}}^{-\frac{1}{2}}(\mathrm{div}_\Gamma, \Gamma_E)$ defined in analogy to (15). The other building blocks correspond to those in (13):

- The functions $\varphi_M^\ell \in H^1(\Gamma)$, $\ell = 2, \ldots, N_M$, are constant $\equiv 1$ on a single magnetic port Γ_M^ℓ and vanish on all other ports.
- The tangential co-homology vectorfields $\mathbf{c}_2^M, \ldots, \mathbf{c}_{N_E}^M \in \boldsymbol{H}(\mathrm{div}_\Gamma, \Gamma) \cap \mathcal{V}_M$ belong to the Γ_M-relative non-bounding boundaries $\partial\Gamma_E^k$, $k = 2, \ldots, N_E$.
- The functions $\mathbf{t}_M^m$, $m = 1, \ldots, N_T$ are $\frac{\pi}{2}$-rotated versions of $\mathbf{t}_E^m$.

3.4 Construction of tangential co-homology vectorfields

Having settled the case of scalar potentials, we focus on the co-homology vectorfields $\mathbf{c}_2^E, \ldots, \mathbf{c}_{N_M}^E$ and $\mathbf{t}_1^E, \ldots, \mathbf{t}_{N_T}^E$. Their construction obeys an common principle. Each one of them is associated with a Γ_E-relative non-bounding cycle $\partial\Gamma_M^2, \ldots, \partial\Gamma_M^{N_M}$ of class (PE) or $\tau_1, \ldots, \tau_{N_T}$ of class (T), respectively, as we have learned in Section 3.2. There we also identified their *dual cycles* $\gamma_\ell^M = \widehat{\partial\Gamma_M^\ell}$, $\ell = 2, \ldots, N_M$, and $\widehat{\tau_m} = \tau_{N_T - m + 1}$, $m = 1, \ldots, N_T$, see Fig. 5.

Dual cycles, also called "cuts" in this context, are key ingredients for our construction. Write $\mathbf{c}^E \in \{\mathbf{c}_2^E, \ldots, \mathbf{c}_{N_M}^E, \mathbf{t}_1^E, \ldots, \mathbf{t}_{N_T}^E\}$ for a generic tangential co-homology vectorfield in $\mathcal{V}_E$, γ for its associated $\partial\Gamma_E$-relative fundamental cycle, and $\widehat{\gamma} \subset \Gamma_I$ for the corresponding dual cycle. Then we can set

$$\mathbf{c}^E := \begin{cases} \widetilde{\mathbf{grad}_\Gamma}\psi^E \text{ on } \Gamma \setminus \Gamma_M \ , \\ \text{arbitrary on } \Gamma_M \ , \end{cases} \quad \text{with} \quad \begin{array}{l} \psi^E \in H^1(\Gamma \setminus (\Gamma_M \cup \widehat{\gamma})) \ , \\ \psi^E = 0 \text{ on } \Gamma_E \ , \\ [\![\psi^E]\!]_{\widehat{\gamma}} = 1 \ , \end{array} \tag{18}$$

where $[\![\psi]\!]_{\widehat{\gamma}}$ denotes the jump of a function across the oriented curve $\widehat{\gamma}$ and $\widetilde{\mathbf{grad}_\Gamma}$ is the (piecewise) surface gradient on $\Gamma \setminus \widehat{\gamma}$. We have enough flexibility in choosing ψ^E to ensure that $\operatorname{supp} \mathbf{c}^E$ is inside a neighborhood of $\widehat{\gamma}$.

We skip the details of the construction of the co-homology vectorfields $\mathbf{c}_k^M \in \boldsymbol{H}^{-\frac{1}{2}}(\mathrm{div}_\Gamma, \Gamma)$, $k = 2, \ldots, N_E$, for $\mathcal{V}_M$, which follows similar lines and just involves a role reversal of Γ_M and Γ_E, and replacing N_M with N_E and $\mathbf{grad}_\Gamma$ with $\mathbf{curl}_\Gamma$, *cf.* Remark 6

4 Variational Formulations

The evolution of the electric field $\mathbf{E} = \mathbf{E}(\boldsymbol{x}, t)$ and of the magnetic field $\mathbf{H} = \mathbf{H}(\boldsymbol{x}, t)$ in Ω is governed by the transient Maxwell's equations:

$$\begin{aligned} \partial_t(\epsilon\mathbf{E}) \quad & +\sigma\mathbf{E} \quad && -\mathbf{curl}\,\mathbf{H} && = 0 \ , && \text{(AL)} \\ \partial_t(\mu\mathbf{H}) \quad & +\mathbf{curl}\,\mathbf{E} && && = 0 \ . && \text{(FL)} \end{aligned}$$

with uniformly positive, possibly spatially varying material coefficients $\epsilon = \epsilon(\boldsymbol{x})$ and $\mu = \mu(\boldsymbol{x})$, and $\sigma = \sigma(\boldsymbol{x}) \geq 0$. These partial differential equations can be cast in weak form in two different ways. In both cases we take for granted that $\mathbf{E}(t) \in \mathcal{V}_E$ and $\mathbf{H}(t) \in \mathcal{V}_M$ for all times.

4.1 E-based weak formulation

We test Ampere's law (AL) with $\mathbf{E}' \in \mathcal{V}_E$, integrate over Ω and then integrate by parts by (1), which yields

$$\int_\Omega \big(\partial_t(\epsilon\mathbf{E}) + \sigma\mathbf{E}\big)\cdot\mathbf{E}' - \mathbf{H}\cdot\mathbf{curl}\,\mathbf{E}'\,\mathrm{d}\boldsymbol{x} - \int_{\partial\Omega} \boldsymbol{\gamma}_\times\mathbf{H}\cdot\boldsymbol{\gamma}_t\mathbf{E}'\,\mathrm{d}S = 0 \quad \forall\mathbf{E}' \in \mathcal{V}_E\,. \tag{19}$$

Appealing to (16) and (13), we can write

$$\boldsymbol{\gamma}_t\mathbf{E}' = \mathbf{grad}_\Gamma\,\varphi'_E + \sum_{\ell=2}^{N_M}\alpha_\ell\mathbf{c}_\ell^E + \sum_{m=1}^{N_T}\beta_m\mathbf{t}_m^E + \widetilde{\mathbf{m}}'\,; \tag{20}$$

with $\varphi'_E \in \mathcal{S}_E$, $\alpha_\ell, \beta_m \in \mathbb{R}$, $\widetilde{\mathbf{m}}' \in \widetilde{\boldsymbol{H}}^{-\frac{1}{2}}(\mathrm{curl}_\Gamma, \Gamma_M)$, see (15).

We examine the boundary term in (19) and start with the observation that the integrand vanishes on $\Gamma_M \cup \Gamma_E$ so that we can confine integration to Γ_I. Then we plug in the representation (20), note that the contribution $\widetilde{\mathbf{m}}'$ does not matter, and get

$$\int_{\Gamma_I} \boldsymbol{\gamma}_\times\mathbf{H}\cdot\boldsymbol{\gamma}_t\mathbf{E}'\,\mathrm{d}S = \int_{\Gamma_I} \boldsymbol{\gamma}_\times\mathbf{H}\cdot\big(\mathbf{grad}_\Gamma\,\varphi'_E + \sum_{\ell=2}^{N_M}\alpha_\ell\mathbf{c}_\ell^E + \sum_{m=1}^{N_T}\beta_m\mathbf{t}_m^E\big)\,.$$

Next, embarking on "formal computations", we use the integration by parts formula

$$\int_{\Gamma_I} \mathbf{v}\cdot\mathbf{grad}_\Gamma\,\psi\,\mathrm{d}S = -\int_{\Gamma_I}\psi\,\mathrm{div}_\Gamma\mathbf{v}\,\mathrm{d}S + \int_{\partial\Gamma_I}\psi\,(\boldsymbol{n}\times\mathbf{v})\cdot\mathrm{d}s \tag{21}$$

for all $\psi \in H^{\frac{1}{2}}(\Gamma_I)$, $\mathbf{v} \in \boldsymbol{H}^{-\frac{1}{2}}(\mathrm{div}_\Gamma, \Gamma_I)$, which yields a sum of circulation integrals

$$\begin{aligned}\int_{\Gamma_I} \boldsymbol{\gamma}_\times\mathbf{H}\cdot\mathbf{grad}_\Gamma\,\varphi'_E\,\mathrm{d}S &= -\int_{\Gamma_I}\varphi'_E\,\underbrace{\mathrm{div}_\Gamma(\boldsymbol{\gamma}_\times\mathbf{H})}_{=0}\,\mathrm{d}S + \int_{\partial\Gamma_E}\varphi'_E\,\mathbf{H}\cdot\mathrm{d}s\\ &= \sum_{k=1}^{N_E}\varphi'_E|_{\Gamma_E^k}\int_{\partial\Gamma_E^k}\mathbf{H}\cdot\mathrm{d}s\,.\end{aligned} \tag{22}$$

Again, we use integration by parts according to (21) to deal with the contribution of the co-homology vectorfields $\mathbf{c}_\ell^E$ and $\mathbf{t}_m^E$. Parallel to the construction in Section 3.4, we consider a generic co-homology vectorfield $\mathbf{c}^E$ given by the formula from (18). Refer to that formula for notations.

$$\begin{aligned}\int_{\Gamma_I} \boldsymbol{\gamma}_\times\mathbf{H}\cdot\mathbf{c}^E\,\mathrm{d}S &= \int_{\Gamma_I}\boldsymbol{\gamma}_\times\mathbf{H}\cdot\widetilde{\mathbf{grad}_\Gamma\psi^E}\,\mathrm{d}S\\ &= -\int_{\Gamma_I}\underbrace{\mathrm{div}_\Gamma\boldsymbol{\gamma}_\times\mathbf{H}}_{=0}\,\psi^E\,\mathrm{d}S + \int_{\partial(\Gamma_I\setminus\widehat{\gamma})}\psi^E\,\boldsymbol{\gamma}_t\mathbf{H}\cdot\mathrm{d}s\\ &\overset{(*)}{=} \int_{\widehat{\gamma}}[\![\psi^E]\!]_{\widehat{\gamma}}\,\boldsymbol{\gamma}_t\mathbf{H}\cdot\mathrm{d}s = \int_{\widehat{\gamma}}\boldsymbol{\gamma}_t\mathbf{H}\cdot\mathrm{d}s\,,\end{aligned} \tag{23}$$

because $\psi^E\boldsymbol{\gamma}_t\mathbf{H}$ has vanishing tangential component on both $\partial\Gamma_E$ and $\partial\Gamma_M$. We point out that integration in $\int_{\partial(\Gamma_I\setminus\widehat{\gamma}}\ldots$ visits both sides of $\widehat{\gamma}$ which accounts for the emergence of the jump in step $(*)$.

Faraday's law (FL) is kept in "strong form" and just tested with $\mathbf{H}' \in \mathcal{V}_M$. This results in the final $\mathbf{E}$-based spatial variational formulation: seek $\mathbf{E} : [0,T] \to \mathcal{V}_E$, $\mathbf{H} : [0,T] \to \mathcal{V}_M$, such that

$$\begin{aligned}\int_\Omega \big(\partial_t(\epsilon\mathbf{E}) + \sigma\mathbf{E}\big)\cdot\mathbf{E}' - \mathbf{H}\cdot\mathbf{curl}\,\mathbf{E}'\,\mathrm{d}\boldsymbol{x} - \sum_{k=2}^{N_E} \varphi_E'|_{\Gamma_E^k} \int_{\partial\Gamma_E^k} \mathbf{H}\cdot\mathrm{d}s \\ - \sum_{\ell=2}^{N_M} \alpha_\ell \int_{\gamma_\ell^M} \boldsymbol{\gamma_t}\mathbf{H}\cdot\mathrm{d}s - \sum_{m=1}^{N_T} \beta_m \int_{\widehat{\tau}_m} \boldsymbol{\gamma_t}\mathbf{H}\cdot\mathrm{d}s = 0\,, \qquad (24)\\ \int_\Omega \big(\partial_t(\mu\mathbf{H}) + \mathbf{curl}\,\mathbf{E}\big)\cdot\mathbf{H}'\,\mathrm{d}\boldsymbol{x} = 0\end{aligned}$$

for all $\mathbf{E}' \in \mathcal{V}_E$ with $\boldsymbol{\gamma_t}\mathbf{E}'$ according to (20), and for all $\mathbf{H}' \in \mathcal{V}_M$. We point out that the dualities (11) have been used to rewrite the circulation integrals.

4.2 H-based variational formulation

Now, we test Faraday's law (FL) with $\mathbf{H}' \in \mathcal{V}_M$ and, after integration by parts, arrive at

$$\int_\Omega \partial_t(\mu\mathbf{H})\cdot\mathbf{H}' + \mathbf{E}\cdot\mathbf{curl}\,\mathbf{H}'\,\mathrm{d}\boldsymbol{x} - \int_\Gamma \boldsymbol{\gamma_t}\mathbf{E}\cdot\boldsymbol{\gamma}_\times\mathbf{H}'\,\mathrm{d}S = 0 \quad \forall \mathbf{H}' \in \mathcal{V}_M\,. \qquad (25)$$

For the rotated tangential trace of the test field we use the representation from (16):

$$\boldsymbol{\gamma}_\times\mathbf{H}' = \mathbf{curl}_\Gamma\varphi_M' + \sum_{k=2}^{N_E}\alpha_k\mathbf{c}_k^M + \sum_{m=1}^{N_T}\beta_m\mathbf{t}_m^M + \widetilde{\mathbf{j}}'\,, \qquad (26)$$

where $\varphi_M' \in \mathcal{S}_M$, $\alpha_k, \beta_m \in \mathbb{R}$, and $\widetilde{\mathbf{j}} \in \widetilde{\boldsymbol{H}}^{-\frac{1}{2}}(\mathrm{div}_\Gamma, \Gamma_E)$. Parallel to the developments of Section 4.1 we can convert the boundary term into

$$\int_\Gamma \boldsymbol{\gamma_t}\mathbf{E}\cdot\mathbf{curl}_\Gamma\varphi_M'\,\mathrm{d}S = \sum_{\ell=1}^{N_M}\varphi_M'|_{\Gamma_M^\ell}\int_{\partial\Gamma_M^\ell}\mathbf{E}\cdot\mathrm{d}s\,, \qquad (27)$$

$$\int_\Gamma \boldsymbol{\gamma_t}\mathbf{E}\cdot\mathbf{c}_k^M\,\mathrm{d}S = \int_{\partial\Gamma_E^k}\boldsymbol{\gamma_t}\mathbf{E}\cdot\mathrm{d}s \quad , \quad \int_\Gamma \boldsymbol{\gamma_t}\mathbf{E}\cdot\mathbf{t}_m^M\,\mathrm{d}S = \int_{\widehat{\tau}_m}\boldsymbol{\gamma_t}\mathbf{E}\cdot\mathrm{d}s\,. \qquad (28)$$

This yields the so-called $\mathbf{H}$-based variational formulation, which involves Ampere's law (AL) in strong form: seek $\mathbf{E} : [0,T] \to \mathcal{V}_E$ and $\mathbf{H} : [0,T] \to \mathcal{V}_M$ such that

$$\begin{aligned}\int_\Omega \big(\partial_t(\epsilon\mathbf{E}) + \sigma\mathbf{E}\big)\cdot\mathbf{E}' - \mathbf{curl}\,\mathbf{H}\cdot\mathbf{E}'\,\mathrm{d}\boldsymbol{x} = 0\,,\\ \int_\Omega \partial_t(\mu\mathbf{H})\cdot\mathbf{H}' + \mathbf{E}\cdot\mathbf{curl}\,\mathbf{H}'\,\mathrm{d}\boldsymbol{x} - \sum_{\ell=1}^{N_M}\varphi_M'|_{\Gamma_M^\ell}\int_{\partial\Gamma_M^\ell}\mathbf{E}\cdot\mathrm{d}s - \qquad (29)\\ \sum_{k=2}^{N_E}\alpha_k\int_{\partial\Gamma_E^k}\boldsymbol{\gamma_t}\mathbf{E}\cdot\mathrm{d}s - \sum_{m=1}^{N_T}\beta_m\int_{\widehat{\tau}_m}\boldsymbol{\gamma_t}\mathbf{E}\cdot\mathrm{d}s = 0\,,\end{aligned}$$

for all $\mathbf{E}' \in \mathcal{V}_E$ and $\mathbf{H}' \in \mathcal{V}_M$. For the latter we have plugged in the representation (26).

Remark 9. If $\Gamma_R \neq \emptyset$, the impedance boundary conditions give rise to extra terms

$$\int_{\Gamma_R} \big(\mathsf{Z}^{-1}(\boldsymbol{\gamma_t}\mathbf{E})\big)(t) \cdot \boldsymbol{\gamma_t}\mathbf{E}' \,\mathrm{d}S \quad \text{and} \quad \int_{\Gamma_R} \big(\mathsf{Z}(\boldsymbol{\gamma}_\times\mathbf{H})\big)(t) \cdot \boldsymbol{\gamma_t}\mathbf{H}' \,\mathrm{d}S \tag{30}$$

entering the first equation of (24) and (29), respectively.

5 Port Conditions

The electric and magnetic time-dependent port quantities in circuit models are

- The **electric potentials** $U_k = U_k(t)$ at the electric ports Γ_E^k, $k = 2, \ldots, N_E$, Γ_E^1 assumed to be grounded.
- The **electric currents** $J_k = J_K(t)$ at the electric ports Γ_E^k, $k = 1, \ldots, N_E$. Their sum is zero.
- The **magnetomotive forces** (M.M.F.) $F_\ell = F_\ell(t)$ at the magnetic ports Γ_M^ℓ, $\ell = 2, \ldots, N_M$, Γ_M^1 as reference.
- The **magnetic fluxes** $\dot{B}_\ell = \dot{B}_\ell(t)$ at the magnetic ports, $\ell = 2, \ldots, N_M$. Those add to zero.
- The **linked magnetic fluxes** $\dot{B}_m^T = \dot{B}_m(t)$, $m = 1, \ldots, N_T$, for loops of the circuit domain Ω_C.
- The **linked electric currents** $J_m^T = J_m^T(t)$, $m = 1, \ldots, N_T$, associated with loops of Ω_C, too.

We hark back to the representations of traces:

$$(13) \quad \Rightarrow \qquad \boldsymbol{\gamma_t}\mathbf{E}(t) = \mathbf{grad}_\Gamma \,\varphi_E(t) + \sum_{\ell=2}^{N_M} \alpha_\ell^E(t)\mathbf{c}_\ell^E + \sum_{m=1}^{N_T} \beta_m^E(t)\mathbf{t}_m^E + \widetilde{\mathbf{m}}(t)\,; \tag{31}$$

$$(16) \quad \Rightarrow \qquad \boldsymbol{\gamma}_\times\mathbf{H}(t) = \mathbf{curl}_\Gamma\varphi_M(t) + \sum_{k=2}^{N_E} \alpha_k^M(t)\mathbf{c}_k^M + \sum_{m=1}^{N_T} \beta_m^M(t)\mathbf{t}_m^M + \widetilde{\mathbf{j}}(t)\,. \tag{32}$$

From them and Maxwell's equations we extract a comprehensive set of expressions for the port quantities, for

$$\text{port voltages:} \qquad U_k(t) = \varphi_E(t)|_{\Gamma_E^k} = \int_{\widehat{\gamma}_k^M = \gamma_k^E} \mathbf{E}(t) \cdot \mathrm{d}s\,, \tag{33a}$$

$$\text{port currents:} \qquad J_k(t) = \alpha_k^M(t) = \int_{\partial\Gamma_E^k} \mathbf{H}(t) \cdot \mathrm{d}s\,, \tag{33b}$$

$$\text{port M.M.F.:} \qquad F_\ell(t) = \varphi_M(t)|_{\Gamma_\ell^M} = \int_{\widehat{\gamma}_\ell^E = \gamma_M^\ell} \mathbf{H}(t) \cdot \mathrm{d}s\,, \tag{33c}$$

$$\text{port magnetic fluxes:} \qquad \dot{B}_\ell(t) = \alpha_\ell^E(t) = \int_{\partial\Gamma_M^\ell} \mathbf{E}(t) \cdot \mathrm{d}s\,, \tag{33d}$$

$$\text{linked magnetic fluxes:} \qquad \dot{B}_m^T(t) = \beta_m^E(t) = \int_{\widehat{\tau}_m} \mathbf{E}(t) \cdot \mathrm{d}s\,, \tag{33e}$$

$$\text{linked electric currents:} \qquad J_m^T(t) = \beta_m^M(t) = \int_{\widehat{\tau}_m} \mathbf{H}(t) \cdot \mathrm{d}s\,, \tag{33f}$$

for all $k = 2, \ldots, N_E$, $\ell = 2, \ldots, N_M$, $m = 1, \ldots, N_T$. The formulas in the left column we may call *essential port conditions*, because they are directly imposed on the fields through (31) and (32), whereas the formulas in the right column may be called *weak port conditions*, because they permit us to enforce them in a variational sense.

Remark 10. For the port quantities (33) the indices k and ℓ run from 2. Don't we neglect fluxes, thus? No, because owing to $\operatorname{div}\mathbf{curl}\,\mathbf{H} = \operatorname{div}\mathbf{curl}\,\mathbf{E} = 0$, and the boundary conditions inherent in $\mathcal{V}_E/\mathcal{V}_M$ we find the flux balance law

$$\sum_{k=1}^{N_E} \int_{\partial\Gamma_E^k} \mathbf{H}(t) \cdot \mathrm{d}s = \sum_{\ell=1}^{N_M} \int_{\partial\Gamma_M^\ell} \mathbf{E}(t) \cdot \mathrm{d}s = 0 \,, \tag{34}$$

which makes it possible to recover the "missing flux" from the others.

In order to endow port conditions with their "natural meaning" in circuit theory we have to impose constraints on the cycles:

(I) The concept of generic port voltages and port M.M.F.s entails the existence of global electric and magnetic scalar potentials, which, however, cannot be reconciled with non-zero linked fluxed given as circulations along topological cycles τ_m, $m-1, \ldots, N_T$. This difficulty can be resolved by treating the tological cycles as "cuts", which render $\Gamma \setminus \bigcup_m \tau_m$ topologically trivial. Therefore, once we restrict all connector cycles to that complement, path integrals along them define meaningful voltages/M.M.F.s.

Assumption 11. *None of the connector cycles $\gamma_1^E, \ldots, \gamma_{N_E}^E$ and $\gamma_1^M, \ldots, \gamma_{N_M}^M$ intersects any of the topological cycles $\tau_1, \ldots, \tau_{N_T}$.*

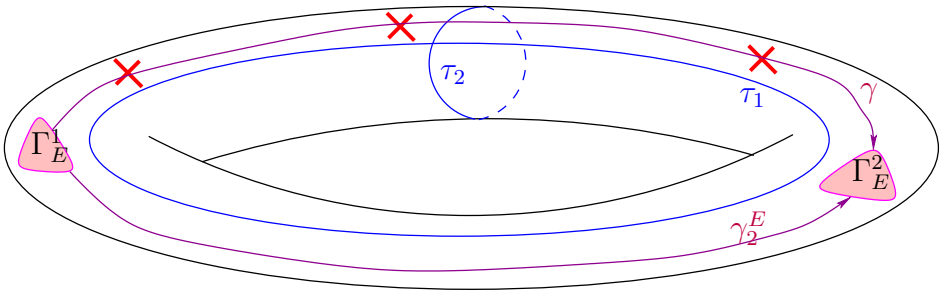

Figure 7: Torus-shaped Ω_C with two electric ports, $N_T = 2$, $N_E = 2$: The connector cycle γ_2^E stays clear of the topological cycles and fulfills Assumption 11, whereas γ is not admissible given how τ_2 is chosen.

We can always find connector cycles with this property, because $\Gamma \setminus \bigcup_m \tau_m$ is still connected. The arrangements displayed in Fig. 4 and Fig. 5 comply with Assumption 11, and another illustration is given in Fig. 7.

The reader must be aware that in the case $N_T > 0$ the choice of the connector cycle is a modeling decision, which will have a big impact on the resulting electromagnetic fields; simulation results covered in Section 7 will demonstrate this.

(II) We have already taken for granted that the "topological cycles" τ_m, $m = 1, \ldots, N_T$, come in dual pairs, recall Section 3.2. They are needed to define the linked fluxes $\dot{B}_m^T$ and currents J_m^T as non-local coupling quantities in (33e) and (33f). In order to give these quantities their "natural meaning", we have to make the following assumption:

Assumption 12. *Half of the cycles τ_m are bounding with respect to Ω_C, whereas their duals are bounding with respect to Ω.*

In fact, this "assumption" could also have been labeled a proposition, because we can always obtain the topological cycles as boundaries of $N_T/2$ "cuts" in Ω_C and Ω, respectively [6, 8, 14]. In [15] it was established that these cuts can be chosen so that they come in pairs whose boundaries constitute dual topological cycles.

Summing up, Assumption 12 will permit us to view $\dot{B}_m^T$ as the electromotive force around a loop of Ω_C and J_m^T the current flowing in a section of it. For an in-depth discussion of this classification of topological cycles refer to [10].

5.1 Ports in E-based Model (24)

In light of the definition (2) of $\mathcal{V}_E$ and (31) we write the time-dependent electric field $\mathbf{E} = \mathbf{E}(t)$ as direct sum (Colors indicate the related cycle classes as in Section 3.2.)

$$\mathbf{E}(t) = \mathbf{E}_0(t) + \mathbf{grad}(\mathsf{X}\rho_E(t)) + \sum_{k=2}^{N_E} U_k(t)\,\mathbf{grad}\,\mathsf{X}\nu_E^k + \sum_{\ell=2}^{N_M} \dot{B}_\ell(t)\mathbf{C}_\ell^E + \sum_{m=1}^{N_T} \dot{B}_m^T(t)\mathbf{T}_m^E \ , \quad (35)$$

where

- $\mathbf{E}_0(t) \in \boldsymbol{H}_{\Gamma\setminus\Gamma_M}(\mathbf{curl},\Omega) := \{\mathbf{V} \in \boldsymbol{H}(\mathbf{curl},\Omega) : \boldsymbol{\gamma_t}\mathbf{V} = 0 \text{ on } \Gamma \setminus \Gamma_M\}$ is the electric field in the interior of the field domain Ω,
- $\rho_E(t) \in \widetilde{H}^{1/2}_{\Gamma_E}(\Gamma_I) := \{\psi \in H^{\frac{1}{2}}(\Gamma_I \cup \Gamma_E) : \psi = 0 \text{ on } \Gamma_E\}$ is the scalar surface potential on the insulating parts of the boundary,
- $\mathsf{X} : H^{\frac{1}{2}}(\Gamma_I \cup \Gamma_E) \to H^1(\Omega)$ is a continuous extension operator,
- $\nu_E^k \in H^{\frac{1}{2}}(\partial\Omega)$ satisfies $\nu_E^k\big|_{\Gamma_E^k} \equiv 1$, $\nu_E^k\big|_{\Gamma_E^m} = 0$ for $m \neq k$, that is, the function ν_E^k attains the value 1 on the electric port Γ_E^k, is "continuous", and vanishes on all other ports,
- $\mathbf{C}_\ell^E \in \boldsymbol{H}(\mathbf{curl},\Omega)$, is an extension of the co-homology tangential surface vector-field $\mathbf{c}_\ell^E$ into Ω, $\ell = 2,\dots,N_M$,
- $\mathbf{T}_m^E \in \boldsymbol{H}(\mathbf{curl},\Omega)$ extends $\mathbf{t}_m^E$: $\boldsymbol{\gamma_t}\mathbf{T}_m^E = \mathbf{t}_m^E$, $m = 1,\dots,N_T$.

Next, we use the "weak expressions" for the port currents J_k from (33b), for the magnetomotive forces F_ℓ from (33c), and for the linked currents from (33f) to replace the special integrals in (24):

$$\int_{\partial\Gamma_E^k} \mathbf{H}\cdot\mathrm{d}s \ \longrightarrow\ J_k \ , \quad \int_{\widehat{\gamma}_\ell^E} \boldsymbol{\gamma_t}\mathbf{H}\cdot\mathrm{d}s \ \longrightarrow\ F_\ell \ , \quad \int_{\widehat{\tau}_m} \boldsymbol{\gamma_t}\mathbf{H}\cdot\mathrm{d}s \ \longrightarrow\ J_m^T \ . \quad (36)$$

Another change compared to (24) is that we relax the smoothness requirements for the magnetic field to $\mathbf{H}(t) \in \boldsymbol{L}^2(\Omega)$ and also $\mathbf{H}' \in \boldsymbol{L}^2(\Omega)$, because no extra regularity is required to render the variational formulation well-defined.

As already done in the derivation of (24), the splitting (35) is also applied to the test field $\mathbf{E}'$, and this yields

(i) two variational equations corresponding to testing with $\mathbf{E}_0' \in \boldsymbol{H}_{\Gamma\setminus\Gamma_M}(\mathbf{curl},\Omega)$ and $\rho_E' \in \widetilde{H}^{1/2}_{\Gamma_E}(\Gamma_I)$,

(ii) and, from (10), $N := N_T + \max\{N_M, 1\} + \max\{N_E, 1\} - 2$ equations from testing with $\mathbf{grad}\,\mathsf{X}\nu_E^k$, $\mathbf{C}_\ell^E$, and $\mathbf{T}_m^E$, $k = 2, \dots, N_E$, $\ell = 2, \dots, N_M$, $m = 1, \dots, N_T$.

Eventually, we end up with the variational problem:

Seek $\mathbf{E}_0 : [0,T] \to \boldsymbol{H}_{\Gamma\setminus\Gamma_M}(\mathbf{curl}, \Omega)$, $\rho_E : [0,T] \to \widetilde{H}^{1/2}_{\Gamma_E}(\Gamma_I)$, $U_k : [0,T] \to \mathbb{R}$, $\dot{B}_\ell : [0,T] \to \mathbb{R}$, $U_k; [0,T] \to \mathbb{R}$, $F_\ell : [0,T] \to \mathbb{R}$, $\dot{B}_m^T : [0,T] \to \mathbb{R}$, $\mathbf{H} : [0,T] \to \boldsymbol{L}^2(\Omega)$ such that

$$\int_\Omega \big(\partial_t(\epsilon\mathbf{E})(t) + \sigma\mathbf{E}(t)\big) \cdot \mathbf{E}_0' - \mathbf{H}(t) \cdot \mathbf{curl}\,\mathbf{E}_0' \,\mathrm{d}\boldsymbol{x} = 0\,, \tag{37a}$$

$$\int_\Omega \big(\partial_t(\epsilon\mathbf{E})(t) + \sigma\mathbf{E}(t)\big) \cdot \mathbf{grad}\,\mathsf{X}\rho_E' \,\mathrm{d}\boldsymbol{x} = 0\,, \tag{37b}$$

$$\int_\Omega \big(\partial_t(\epsilon\mathbf{E})(t) + \sigma\mathbf{E}(t)\big) \cdot \mathbf{grad}\,\mathsf{X}\nu_E^k \,\mathrm{d}\boldsymbol{x} - J_k(t) = 0\,, \tag{37c}$$

$$\int_\Omega \big(\partial_t(\epsilon\mathbf{E})(t) + \sigma\mathbf{E}(t)\big) \cdot \mathbf{C}_\ell^E - \mathbf{H}(t) \cdot \mathbf{curl}\,\mathbf{C}_\ell^E \,\mathrm{d}\boldsymbol{x} - F_\ell(t) = 0\,, \tag{37d}$$

$$\int_\Omega \big(\partial_t(\epsilon\mathbf{E})(t) + \sigma\mathbf{E}(t)\big) \cdot \mathbf{T}_m^E - \mathbf{H}(t) \cdot \mathbf{curl}\,\mathbf{T}_m^E \,\mathrm{d}\boldsymbol{x} - J_m^T(t) = 0\,, \tag{37e}$$

$$\int_\Omega \big(\partial_t(\mu\mathbf{H})(t) + \mathbf{curl}\,\mathbf{E}(t)\big) \cdot \mathbf{H}' \,\mathrm{d}\boldsymbol{x} = 0 \tag{37f}$$

for all $\mathbf{E}_0' \in \boldsymbol{H}_{\Gamma\setminus\Gamma_M}(\mathbf{curl}, \Omega)$, $\rho_E' \in \widetilde{H}^{1/2}_{\Gamma_E}(\Gamma_I)$, $k = 2, \dots, N_E$, $\ell = 2, \dots, N_M$, $m = 1, \dots, N_T$, and $\mathbf{H}' \in \boldsymbol{L}^2(\Omega)$.

Note that in (37) $\mathbf{E}$ has to be read as an expression depending affine-linearly on $\mathbf{E}_0$, ρ_E, U_k,$\dot{B}_\ell$, and $\dot{B}_m^T$ according to (35).

Formally, there is a mismatch of the number of equations and unknowns in (37) ("Six equations for nine unknowns"), which leaves freedom to imposed values for port quantities or relationships between them. This is how we can introduce sources and circuit relations into the model.

Remark 13 (Elimination of magnetic field)**.** Assume that none of the material coefficients ϵ, σ, and μ depends on time. Then we can

1. differentiate (37a)–(37e) with respect to time t, which amounts to replacing
$$\partial(\epsilon\mathbf{E})(t) \to \epsilon\partial_t^2\mathbf{E}(t)\,, \quad \sigma\mathbf{E}(t) \to \sigma\partial_t\mathbf{E}(t)\,, \quad \mathbf{H}(t) \to \partial_t\mathbf{H}(t)\,.$$
2. move ∂_t right in front of $\mathbf{H}$ in (37f): $\partial_t(\mu\mathbf{H})(t) \to \mu\partial_t\mathbf{H}$.

Subsequently, we can test (37e) with $\mu^{-1}\,\mathbf{curl}\,\mathbf{E}_0'$, $\mu^{-1}\,\mathbf{curl}\,\mathbf{C}_\ell^E$, and $\mu^{-1}\,\mathbf{curl}\,\mathbf{T}_m^E$, respectively, and use the resulting equation to eliminate $\mathbf{H}(t)$ in (37a), (37d), and (37e). We end up with an evolution equation for the electric field $\mathbf{E}$ alone, second-order in time, which retains all the coupling quantities.

5.2 Ports in H-Based Model (29)

Of course, the approach to (29) runs parallel to the developments of Section 5.1. From (3)/(32) we get the direct-sum representation

$$\mathbf{H}(t) = \mathbf{H}_0(t) + \mathbf{grad}\,\mathsf{X}\rho_M(t) + \sum_{\ell=2}^{N_M} F_\ell(t)\,\mathbf{grad}\,\mathsf{X}\nu_M^\ell + \sum_{k=2}^{N_E} J_k(t)\mathbf{C}_k^M + \sum_{m=1}^{N_T} J_m^T(t)\mathbf{T}_m^M\,, \tag{38}$$

where

- $\mathbf{H}_0(t) \in \boldsymbol{H}_{\Gamma\setminus\Gamma_E}(\mathbf{curl},\Omega) := \{\mathbf{V} \in \boldsymbol{H}(\mathbf{curl},\Omega) : \boldsymbol{\gamma}_\times\mathbf{V} = 0 \text{ on } \Gamma\setminus\Gamma_E\}$ is the magnetic field in the interior of Ω and at the electric ports,
- $\rho_M(t) \in \widetilde{H}^{1/2}_{\Gamma_M}(\Gamma_I) := \{\psi \in H^{\frac{1}{2}}(\Gamma_I\cup\Gamma_M) : \psi = 0 \text{ on } \Gamma_M\}$ is a magnetic scalar surface potential on Γ_I,
- $\nu^\ell_M \in H^{\frac{1}{2}}(\partial\Omega)$ is equal to 1 on Γ^ℓ_M, and zero on all other magnetic parts and all electric ports.
- $\mathbf{C}^M_k \in \boldsymbol{H}(\mathbf{curl},\Omega)$ extends the surface co-homology vectorfield $\mathbf{c}^M_k$: $\boldsymbol{\gamma}_\times\mathbf{C}^M_k = \mathbf{c}^M_k$, $k = 2,\ldots,N_E$.
- $\mathbf{T}^M_m$ is an $\boldsymbol{H}(\mathbf{curl},\Omega)$-extension of $\mathbf{t}^H_m$: $\boldsymbol{\gamma}_\times\mathbf{T}^M_m = \mathbf{t}^M_m$.

The expressions (33d) and (33a) allow the following replacements of integral expressions in (29):

$$\int_{\partial\Gamma^\ell_M}\mathbf{E}\cdot\mathrm{d}s \;\longrightarrow\; \dot{B}_\ell\,,\quad \int_{\gamma^M_k}\boldsymbol{\gamma_t}\mathbf{E}\cdot\mathrm{d}s \;\longrightarrow\; U_k\,,\quad \int_{\widehat{\tau}_m}\boldsymbol{\gamma_t}\mathbf{E}\cdot\mathrm{d}s \;\longrightarrow\; \dot{B}^T_m\,. \tag{39}$$

As before, the smoothness requirements for $\mathbf{E}$ and $\mathbf{E}'$ in (29) are relaxed and we merely demand $\mathbf{E},\mathbf{E}' \in \boldsymbol{L}^2(\Omega)$. This leads to the final $\mathbf{H}$-based variational formulation taking into account port quantitites:

Seek $\mathbf{H}_0 : [0,T] \to \boldsymbol{H}_{\Gamma\setminus\Gamma_E}(\mathbf{curl},\Omega)$, $\rho_M : [0,T] \to \widetilde{H}^{1/2}_{\Gamma_M}(\Gamma_I)$, $F_\ell : [0,T] \to \mathbb{R}$, $J_k : [0,T] \to \mathbb{R}$, $J^T_m : [0,T] \to \mathbb{R}$, $\mathbf{H} : [0,T] \to \boldsymbol{L}^2(\Omega)$

$$\int_\Omega \partial_t(\mu\mathbf{H})(t)\cdot\mathbf{H}'_0 + \mathbf{E}(t)\cdot\mathbf{curl}\,\mathbf{H}'_0\,\mathrm{d}\boldsymbol{x} = 0\,, \tag{40a}$$

$$\int_\Omega \partial_t(\mu\mathbf{H})(t)\cdot\mathbf{grad}\,\mathsf{X}\rho'_M\,\mathrm{d}\boldsymbol{x} = 0\,, \tag{40b}$$

$$\int_\Omega \partial_t(\mu\mathbf{H})(t)\cdot\mathbf{grad}\,\mathsf{X}\nu^\ell_M\,\mathrm{d}\boldsymbol{x} - \dot{B}_\ell(t) = 0\,, \tag{40c}$$

$$\int_\Omega \partial_t(\mu\mathbf{H})(t)\cdot\mathbf{C}^k_M + \mathbf{E}\cdot\mathbf{curl}\,\mathbf{C}^k_M\,\mathrm{d}\boldsymbol{x} - U_k(t) = 0\,, \tag{40d}$$

$$\int_\Omega \partial_t(\mu\mathbf{H})(t)\cdot\mathbf{T}^m_M + \mathbf{E}(t)\cdot\mathbf{curl}\,\mathbf{T}^m_M\,\mathrm{d}\boldsymbol{x} - \dot{B}^T_m(t) = 0\,, \tag{40e}$$

$$\int_\Omega \big(\partial_t(\epsilon\mathbf{E})(t) + \sigma\mathbf{E}(t)\big)\cdot\mathbf{E}' - \mathbf{curl}\,\mathbf{H}(t)\cdot\mathbf{E}'\,\mathrm{d}\boldsymbol{x} = 0 \tag{40f}$$

for all $\mathbf{H}'_0 \in \boldsymbol{H}(\mathrm{curl}_\Gamma,\Gamma)\Gamma\setminus\Gamma_E$, $\rho'_M \in \widetilde{H}^{1/2}_{\Gamma_M}(\Gamma_I)$, $\ell = 1,\ldots,N_M$, $k = 2,\ldots,N_E$, $m = 1,\ldots,N_T$, $\mathbf{E}' \in \boldsymbol{L}^2(\Omega)$, and $\mathbf{H} = \mathbf{H}(\mathbf{H}_0,\rho_M,F_\ell,J_k,J^T_m)$ as in (38).

Also here we face "six equations versus nine unknowns" and either fixing port quantities, aka, imposing excitation through sources, or adding circuit equations will remedy this imbalance. I goes without saying that here we can eliminate the electric field $\mathbf{E}$, *cf.* Remark 13.

5.3 Power Balance

Conservation of energy is a guiding principle in the coupling of fields and circuits [1, 11]. It is also respected in the variational formulations (37) and (40). We elaborate this for the $\mathbf{E}$-based formulation (37).

The idea is to set $\mathbf{E}' := \mathbf{E}(t)$ and $\mathbf{H}' := \mathbf{H}(t)$ in (24) and add both resulting equations taking into account (33) and (35)

$$J_k(t) = \int_{\partial\Gamma_E^k} \mathbf{H}(t)\cdot \mathrm{d}s\ , \quad F_\ell(t) = \int_{\widehat{\gamma}_\ell^E} \mathbf{H}(t)\cdot \mathrm{d}s\ , \quad J_m^T(t) = \int_{\widehat{\tau}_m} \mathbf{H}(t)\cdot \mathrm{d}s\ .$$

This gives us the power balance relation

$$\begin{aligned}\frac{d}{dt}\int_\Omega \tfrac{1}{2}\epsilon\mathbf{E}(t)\cdot\mathbf{E}(t) + \tfrac{1}{2}\mu\mathbf{H}(t)\cdot\mathbf{H}(t)\,\mathrm{d}\boldsymbol{x} + \int_\Omega \sigma\mathbf{E}(t)\cdot\mathbf{E}(t)\,\mathrm{d}\boldsymbol{x}\\ = \int_\Omega \partial_t(\epsilon\mathbf{E})(t)\cdot\mathbf{E}(t) + \partial_t(\mu\mathbf{H})(t)\cdot\mathbf{H}(t) + \sigma\mathbf{E}(t)\cdot\mathbf{E}(t)\,\mathrm{d}\boldsymbol{x}\\ = \sum_{k=1}^{N_E} U_k(t)J_k(t) + \sum_{\ell=1}^{\beta_M} \dot{B}_\ell(t)F_\ell(t) + \sum_{m=1}^{N_T} J_m^T(t)\dot{B}_m^T(t)\ . \quad (41)\end{aligned}$$

The products of the port quantities give the power flux through each port, which is offset by a change in the electromagnetic field energies and Ohmic losses. The same argument can be made for the **H**-based model.

Remark 14. In the case $\Gamma_R \neq \emptyset$ another term of the form

$$\int_{\Gamma_R} \big(\mathsf{Z}^{-1}(\boldsymbol{\gamma}_t\mathbf{E})\big)(t)\cdot\boldsymbol{\gamma}_t\mathbf{E}(t)\,\mathrm{d}S = \int_{\Gamma_R} \big(\mathsf{Z}(\boldsymbol{\gamma}_\times\mathbf{H})\big)(t)\cdot\boldsymbol{\gamma}_\times\mathbf{H}(t)\,\mathrm{d}S \quad (42)$$

emerges on the right-hand side of (41). Straightforwardly, it arises from (30). It represents the power carried off by electromagnetic radiation.

6 Finite-Element Exterior Calculus (FEEC) Discretization

The variational problems (37) and (40) immediately lend themselves to a Galerkin discretization by means of discrete differential forms on a tetrahedral mesh $\mathcal{M}$ of Ω, which *resolve the ports* in the sense that every Γ_E^k and Γ_M^ℓ is the union of faces of mesh cells. All geometric entities of the mesh are to be endowed with an intrinsic orientation.

We restrict the discussion to the **E**-based model (37) and leave the analogous considerations for the **H**-based model (40) to the reader. We also focus on lowest-order FEEC approximation, known as edge elements/Whitney-1-forms in the case of finite-element subspaces of $\boldsymbol{H}(\mathbf{curl},\Omega)$ [9, Sect. 3]. Their locally supported basis functions, dubbed "edge basis functions" in the sequel, are associated with edges of $\mathcal{M}$. We remind that FEEC offers discrete potentials and the relevant discrete scalar potentials are provided by $\mathcal{M}$-piecewise linear continuous functions. Those can be written as linear combinations of node-associated locally supported basis functions. We refer to them as "tent functions".

The following finite-dimensional trial and test space can be used in (37):

- $\boldsymbol{H}_{\Gamma\setminus\Gamma_M}(\mathbf{curl},\Omega)$ is replaced with the space $\mathcal{E}_h$ spanned by edge basis functions associated with Ω-interior edges of $\mathcal{M}$ plus edges in the interior of magnetic ports.
- The finite element subspace of $\widetilde{H}^{1/2}_{\Gamma_E}(\Gamma_I)$ is generated by the traces of those tent functions belonging to the nodes located in the interior of Γ_I and on $\partial\Gamma_M$. We write $\mathcal{S}_h$ for their span.

- For the finite-element approximation of $\boldsymbol{L}^2(\Omega)$ we simply use the space $\mathcal{C}_h$ of $\mathcal{M}$-piecewise constant vectorfields.

The equations (37b) and (37c) feature the extension operator X. In the finite-element setting we use simple nodal truncation: extension of a $\mathcal{M}|_\Gamma$-piecewise linear function is done by keeping all nodal values on Γ and setting the contributions of all tent functions at nodes in the interior of Ω to zero.

The next isssue is the representation of the special functions ν_E^k and $\mathbf{C}_\ell^M$ occurring in (37c) and (37d), respectively. Those are defined in the paragraph following (35). The function ν_E^k is simply given as the sum of all tent functions belonging to mesh nodes contained in $\overline{\Gamma}_E^k$. Note the closure of the set! The partition-of-unity property of the tent function yields the desired properties of the resulting $\mathcal{M}$-piecewise linear function $\mathsf{X}\nu_E^k$.

The construction of $\mathbf{C}_\ell^E$ and $\mathbf{T}_m^E$ is more challenging. It follows recipes already developed in [10]: As explained in Section 3.4 to every $\mathbf{C}_\ell^E$ there is an associated dual cycle γ_ℓ^M of class (CM), which is an oriented curve. The same applies to every $\mathbf{T}_m^E$ and its dual cycle is also of class (T).

Assumption 15. *We assume that every cycle γ_ℓ^M, $\ell = 2, \ldots, N_M$, γ_k^E, $k = 2, \ldots, N_E$, and τ_m, $m = 1, \ldots, N_T$, is a chain of edges of $\mathcal{M}$.*

This assumption can always be met, provided that the mesh resolves the topology of Ω. Given a dual cycle $\widehat{\gamma}/\widehat{\tau}_m$ as an edge chain $\subset \Gamma$, we can choose the associated co-homology vector fields $\mathbf{c}_\ell^E/\mathbf{t}_m^E$ as so-called collar fields supported in the triangles adjacent to the dual cycle $\widehat{\gamma}$ on "the right side". For details refer to Fig. 8 and [10]. Afterwards we employ simple nodal truncation to extend them to finite-element vectorfields on Ω.

Remark 16. Note that collar fields are extremely sparse under the reasonable assumption that the edge cycles do not behave like surface-filling curves: viewed as finite-element functions only a few degrees of freedom will be non-zero in the edge basis representations of the collar fields.

Then, given the collar fields $\mathbf{c}_\ell^E$, we obtain $\mathbf{C}_\ell^E$ by simply retaining the weights of the edge basis functions on Γ and setting all those for interior edge basis functions to zero, which is the "trivial finite-element extension procedure". The same construction applies to $\mathbf{T}_m^E$.

Finally, let us exhibit the structure of the semi-discrete evolution problem for the **E**-based formulation, an ordinary differential equation for the basis expansion coefficients of the unknown fields plus the port quantities. To that end we introduce the time-dependent coefficient vectors

- $\vec{E} = \vec{E}(t) \in \mathbb{R}^{n_E}$ for the edge-basis expansion coefficients of $\mathbf{E}_{0,h} : [0,T] \to \mathcal{E}_h$,
- $\vec{\rho} = \vec{\rho}(t) \in \mathbb{R}^{n_S}$ for the tent-basis expansion coefficient vector of $\mathsf{X}\rho_{E,h} : [0,T] \to \mathcal{S}_h$,
- $\vec{H} = \vec{H}(t) \in \mathbb{R}^{n_H}$ for the vector of cell values of $\mathbf{H}_h : [0,T] \to \mathcal{C}_h$,
- $\vec{U}(t) := (U_2(t), \ldots, U_{N_E}(t))^\top \in \mathbb{R}^{N_E-1}$,
  $\vec{B}(t) = (\dot{B}_1(t), \ldots, \dot{B}_{N_M-1}(t))^\top \in \mathbb{R}^{N_M-1}$,
  $\vec{L}(t) = (\dot{B}_1^T(t), \ldots, \dot{B}_{N_T}^T(t)) \in \mathbb{R}^{N_T}$,
- $\vec{J}(t) = (J_2(t), \ldots, J_{N_E}(t))^\top \in \mathbb{R}^{N_E-1}$,
  $\vec{F}(t) = (F_2(t), \ldots, F_{N_M}(t))^\top \in \mathbb{R}^{N_M-1}$,
  $\vec{I}(t) = (J_1^T(t), \ldots, J_{N_T}^T(t))^\top \in \mathbb{R}^{N_T}$.

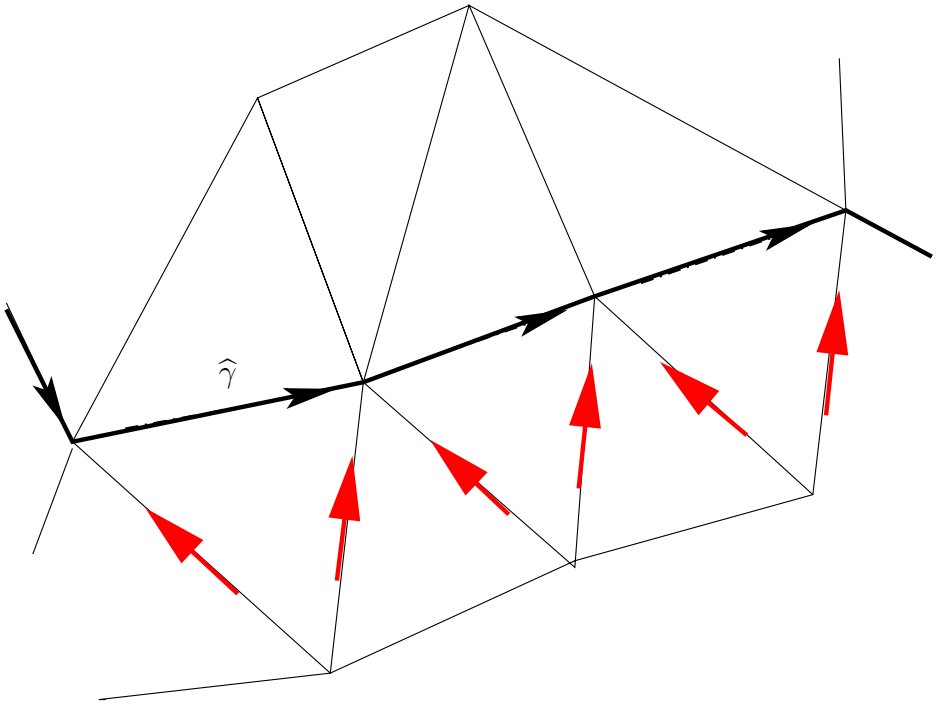

Figure 8: Close-up of the collar field $\mathbf{c}^E$ skirting the dual cycle $\widehat{\gamma}$. The red arrows indicate the edges whose edge basis functions will contribute to $\mathbf{c}^E$ with weight $+1$.

$$\begin{pmatrix} \mathbf{M}_{EE} & \mathbf{M}_{\rho E} & \mathbf{M}_{UE} & \mathbf{M}_{BE} & \mathbf{M}_{LE} & \mathbf{O} \\ \mathbf{M}_{\rho E}^\top & \mathbf{M}_{\rho\rho} & \mathbf{M}_{U\rho} & \mathbf{M}_{B\rho} & \mathbf{M}_{L\rho} & \mathbf{O} \\ \mathbf{M}_{UE}^\top & \mathbf{M}_{U\rho}^\top & \mathbf{M}_{UU} & \mathbf{M}_{BU} & \mathbf{M}_{LU} & \mathbf{O} \\ \mathbf{M}_{BE}^\top & \mathbf{M}_{B\rho}^\top & \mathbf{M}_{BU} & \mathbf{M}_{BB} & \mathbf{M}_{LB} & \mathbf{O} \\ \mathbf{M}_{LE}^\top & \mathbf{M}_{L\rho}^\top & \mathbf{M}_{LU}^\top & \mathbf{M}_{LB}^\top & \mathbf{M}_{LL} & \mathbf{O} \\ \mathbf{O} & \mathbf{O} & \mathbf{O} & \mathbf{O} & \mathbf{O} & \mathbf{M}_{HH} \end{pmatrix} \frac{d}{dt} \begin{pmatrix} \vec{E} \\ \vec{\rho} \\ \vec{U} \\ \vec{B} \\ \vec{L} \\ \vec{H} \end{pmatrix} +$$

$$\begin{pmatrix} \mathbf{R}_{EE} & \mathbf{R}_{\rho E} & \mathbf{R}_{UE} & \mathbf{R}_{BE} & \mathbf{R}_{LE} & \mathbf{O} \\ \mathbf{R}_{\rho E}^\top & \mathbf{R}_{\rho\rho} & \mathbf{R}_{U\rho} & \mathbf{R}_{B\rho} & \mathbf{R}_{L\rho} & \mathbf{O} \\ \mathbf{R}_{UE}^\top & \mathbf{R}_{U\rho}^\top & \mathbf{R}_{UU} & \mathbf{R}_{BU} & \mathbf{R}_{LU} & \mathbf{O} \\ \mathbf{R}_{BE}^\top & \mathbf{R}_{B\rho}^\top & \mathbf{R}_{BU} & \mathbf{R}_{BB} & \mathbf{R}_{LB} & \mathbf{O} \\ \mathbf{R}_{LE}^\top & \mathbf{R}_{L\rho}^\top & \mathbf{R}_{LU}^\top & \mathbf{R}_{LB}^\top & \mathbf{R}_{LL} & \mathbf{O} \\ \mathbf{O} & \mathbf{O} & \mathbf{O} & \mathbf{O} & \mathbf{O} & \mathbf{O} \end{pmatrix} \begin{pmatrix} \vec{E} \\ \vec{\rho} \\ \vec{U} \\ \vec{B} \\ \vec{L} \\ \vec{H} \end{pmatrix} +$$

$$\begin{pmatrix} \mathbf{O} & \mathbf{O} & \mathbf{O} & \mathbf{O} & \mathbf{O} & -\mathbf{C} \\ \mathbf{O} & \mathbf{O} & \mathbf{O} & \mathbf{O} & \mathbf{O} & \mathbf{O} \\ \mathbf{O} & \mathbf{O} & \mathbf{O} & \mathbf{O} & \mathbf{O} & \mathbf{O} \\ \mathbf{O} & \mathbf{O} & \mathbf{O} & \mathbf{O} & \mathbf{O} & -\mathbf{Q} \\ \mathbf{O} & \mathbf{O} & \mathbf{O} & \mathbf{O} & \mathbf{O} & -\mathbf{P} \\ \mathbf{C}^\top & \mathbf{O} & \mathbf{O} & \mathbf{Q}^\top & \mathbf{P}^\top & \mathbf{O} \end{pmatrix} \begin{pmatrix} \vec{E} \\ \vec{\rho} \\ \vec{U} \\ \vec{B} \\ \vec{L} \\ \vec{H} \end{pmatrix} = \begin{pmatrix} 0 \\ 0 \\ \vec{J} \\ \vec{F} \\ \vec{I} \\ 0 \end{pmatrix} .$$

The mass matrices $\mathbf{M}_{**}$, $*, \star \in \{E, \rho, U, B, L\}$ arise from the Galerkin discretization of the bilinear form $(\mathbf{E}, \mathbf{E}') \mapsto \int_\Omega \epsilon(\boldsymbol{x}) \mathbf{E} \cdot \mathbf{E}' \, \mathrm{d}\boldsymbol{x}$, with the exception of $\mathbf{M}_{HH} \in \mathbb{R}^{n_H, n_H}$, which is a discretization of $(\mathbf{H}, \mathbf{H}') \mapsto \int_\Omega \mu(\boldsymbol{x}) \mathbf{H} \cdot \mathbf{H}' \, \mathrm{d}\boldsymbol{x}$ on $\mathcal{C}_h \times \mathcal{C}_h$. The matrices $\mathbf{R}_{**}$, $*, \star \in \{E, \rho, U, B, L\}$ are produced by the Galerkin discretization of the Ohmic loss blinear form $(\mathbf{E}, \mathbf{E}') \mapsto \int_\Omega \sigma(\boldsymbol{x}) \mathbf{E} \cdot \mathbf{E}' \, \mathrm{d}\boldsymbol{x}$ on the spaces indicated by the subscripts.

The matrices $\mathbf{C} \in \mathbb{R}^{n_E, n_H}$ represent a discrete **curl**-operator obtained by the Galerkin discretization of $(\mathbf{H}, \mathbf{E}') \mapsto \int_\Omega \mathbf{H} \cdot \mathbf{curl}\, \mathbf{E}' \, \mathrm{d}\boldsymbol{x}$ on $\mathcal{C}_h \times \mathcal{E}_h$. The entries of the matrix $\mathbf{Q} \in \mathbb{R}^{N_M - 1, n_H}$ arise from pluggin the basis functions of $\mathcal{C}_h$ into the lin-

ear forms $\mathbf{H} \mapsto \int_\Omega \mathbf{H} \cdot \mathbf{curl}\, \mathbf{C}_\ell^E \,\mathrm{d}\boldsymbol{x}$, $\ell = 2, \ldots, N_M$, and we get $\mathbf{P} \in \mathbb{R}^{N_T, n_H}$ from the Galerkin discretization of $(\mathbf{H}, \mathbf{E}') \mapsto \int_\Omega \mathbf{H} \cdot \mathbf{curl}\, \mathbf{E}' \,\mathrm{d}\boldsymbol{x}$ on $\mathcal{C}_h \times \mathrm{span}\{\mathbf{T}_1^E, \ldots, \mathbf{T}_{N_T}^E\}$.

7 Example: E-Based Formulation, Excitation by Linked Flux

We discuss a conrete simulation in *frequency domain* at a fixed frequency $f = \frac{\omega}{2\pi} =$ 50Hz. We rely on the **E**-based model (37) and replace $\partial_t \to \cdot i\omega$ and regard all fields and port quantities as complex-valued phasors. We consider the particular geometry displayed in Fig. 9, which means $N_E = 2$, $N_M = 0$, and $N_T = 2$. Topologically, this resembles the situation of Fig. 7.

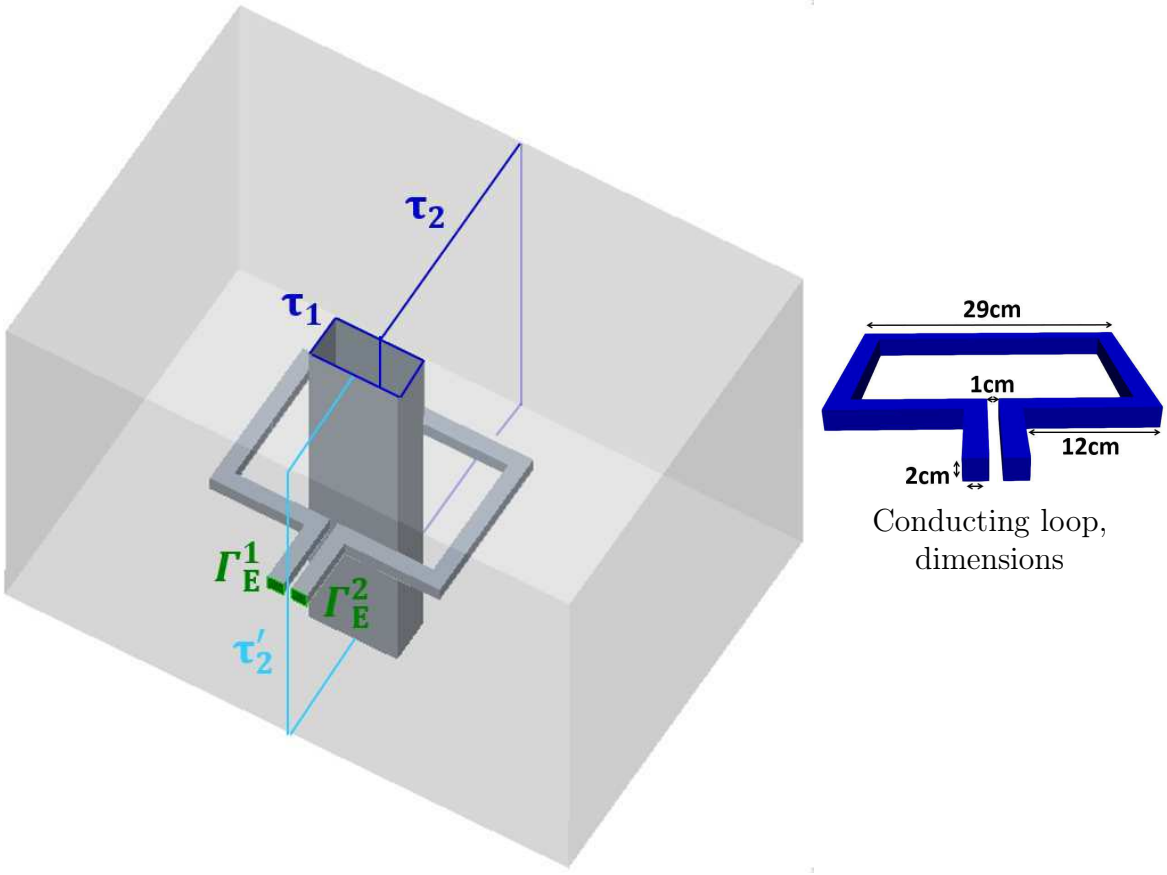

Conducting loop, dimensions

Figure 9: Geometry for numerical demonstration: bounded field domain Ω with the shape of a "cubistic torus" ($N_T = 2$), whose complement represents the unbounded circuit domain Ω_C. Central tunnel surrounded by conducting split loop, connected to two electric ports ($N_E = 2$). Conductivity $\sigma = 10^6$A/Vm inside loop, $\sigma = 0$ outside, $\mu = \mu_0$, $\epsilon = \epsilon_0$ everywhere. The topological cycles τ_1, τ_2 are marked in blue, an alternative topological cycle τ_2' in cyan.

We short-circuit the electric ports, which amounts to imposing $U_2 = 0$ in the notations of Section 5.1 and drive the system by through a linked magnetic flux $\dot{B}_1^T \in \mathbb{C}$ penetrating the surface bounded by τ_1. This is equivalent to imposing an electromotive force along τ_1, see (33e). Such excitation can model the effect of a current-carrying coil outside the field domain.

We end up with a special frequency-domain version of (37). Given $\dot{B}_1^T \in \mathbb{C}$ seek[4]

$$\mathbf{E} = \mathbf{E}_0 + \mathbf{grad}\, \mathsf{X}\rho_E + \dot{B}_1^T \mathbf{T}_1^E + \dot{B}_2^T \mathbf{T}_2^E \quad [\, + U_2\, \mathbf{grad}\, \mathsf{X}\nu_E^2\,] \tag{43}$$

[4]Unknowns are marked with purple color.

with $\mathbf{E}_0 \in \boldsymbol{H}_0(\mathbf{curl}, \Omega)$, $\rho_E \in \widetilde{H}^{1/2}_{\Gamma_E}(\Gamma_I)$, $\dot{B}_2^T \in \mathbb{C}$, and $\mathbf{H} \in \boldsymbol{L}^2(\Omega)$, $J_2^T \in \mathbb{C}$ such that

$$\int_\Omega \big(i\omega\epsilon(\boldsymbol{x}) + \sigma(\boldsymbol{x})\big)\mathbf{E} \cdot \mathbf{E}_0' - \mathbf{H} \cdot \mathbf{curl}\, \mathbf{E}_0' \,\mathrm{d}\boldsymbol{x} = 0\,, \tag{44a}$$

$$\int_\Omega \big(i\omega\epsilon(\boldsymbol{x}) + \sigma(\boldsymbol{x})\big)\mathbf{E} \cdot \mathbf{grad}\, \mathsf{X}\rho_E' \,\mathrm{d}\boldsymbol{x} = 0\,, \tag{44b}$$

$$\int_\Omega \big(i\omega\epsilon(\boldsymbol{x}) + \sigma(\boldsymbol{x})\big)\mathbf{E} \cdot \mathbf{T}_2^E - \mathbf{H} \cdot \mathbf{curl}\, \mathbf{T}_2^E \,\mathrm{d}\boldsymbol{x} - J_2^T = 0\,, \tag{44c}$$

$$\int_\Omega \big(i\omega\mu(\boldsymbol{x})\mathbf{H} + \mathbf{curl}\, \mathbf{E}\big) \cdot \mathbf{H}' \,\mathrm{d}\boldsymbol{x} = 0 \tag{44d}$$

for all $\mathbf{E}_0' \in \boldsymbol{H}_0(\mathbf{curl}, \Omega)$, $\rho_E' \in \widetilde{H}^{1/2}_{\Gamma_E}(\Gamma_I)$, and $\mathbf{H}' \in \boldsymbol{L}^2(\Omega)$. In (43) we have hinted that the voltage drop between the electric ports is imposed, though in this example $U_2 = 0$. This removes a degree of freedom from the trial space for $\mathbf{E}$, which forces us to remove the corresponding one from the test space. As a consequence (37c) does not contribute to the variational equations.

Next, we eliminate the magnetic field $\mathbf{H}$ as discussed in Remark 13 by testing (44d) with $\mathbf{H}' := \mathbf{curl}\, \mathbf{E}_0'$ and $\mathbf{H}' := \mathbf{curl}\, \mathbf{T}_2^E$, respectively, and obtain: Seek $\mathbf{E}$ as defined in (43) and $J_2^T \in \mathbb{C}$ such that

$$\int_\Omega \big(i\omega\epsilon(\boldsymbol{x}) + \sigma(\boldsymbol{x})\big)\mathbf{E} \cdot \mathbf{E}_0' + \frac{1}{i\omega\mu(\boldsymbol{x})}\, \mathbf{curl}\, \mathbf{E} \cdot \mathbf{curl}\, \mathbf{E}_0' \,\mathrm{d}\boldsymbol{x} = 0\,, \tag{45a}$$

$$\int_\Omega \big(i\omega\epsilon(\boldsymbol{x}) + \sigma(\boldsymbol{x})\big)\mathbf{E} \cdot \mathbf{grad}\, \mathsf{X}\rho_E' \,\mathrm{d}\boldsymbol{x} = 0\,, \tag{45b}$$

$$\int_\Omega \big(i\omega\epsilon(\boldsymbol{x}) + \sigma(\boldsymbol{x})\big)\mathbf{E} \cdot \mathbf{T}_2^E + \frac{1}{i\omega\mu(\boldsymbol{x})}\, \mathbf{curl}\, \mathbf{E} \cdot \mathbf{curl}\, \mathbf{T}_2^E \,\mathrm{d}\boldsymbol{x} - J_2^T = 0 \tag{45c}$$

for all $\mathbf{E}_0' \in \boldsymbol{H}_0(\mathbf{curl}, \Omega)$ and $\rho_E' \in \widetilde{H}^{1/2}_{\Gamma_E}(\Gamma_I)$.

The unknown J_2^T represents the complex amplitude of the total current flowing through τ_2, whereas $\dot{B}_2^T$ is the electromotive force around τ_2. The complex amplitude of the current J_2 flowing through the electric ports can be recovered from (37c):

$$J_2 = \int_\Omega \big(i\omega\epsilon(\boldsymbol{x}) + \sigma(\boldsymbol{x})\big)\mathbf{E} \cdot \mathbf{grad}\, \mathsf{X}\nu_E^2 \,\mathrm{d}\boldsymbol{x}\,, \tag{46}$$

where ν_E^2 has been specified in Section 5.1.

The finite-element Galerkin discretization of (45) is carried out precisely as described in Section 6 using three tetrahedral meshes of increasing resolution. The mutually dual topological cycles τ_1 and τ_2 directly enter the model through the co-homology vector fields $\mathbf{T}_1^E$ and $\mathbf{T}_2^E$, which we constructed as "collar fields" skirting the dual cycle according to the algorithm outlined in Fig. 8. We choose both τ_1 and τ_2 as flat rectangles as indicated in Fig. 9. For the cycle τ_2 we explore two options,

(i) the cycle bounds a flat surface cutting the conductor, τ_2 in Fig. 9,

(ii) the cycle runs between the contacts and the associated surface cuts through the air gap of the split conducting loop, τ_2' in Fig. 9.

For both choices we visualize the electric currents in Fig. 10 and tabulate J_2 for different meshes in Table 1.

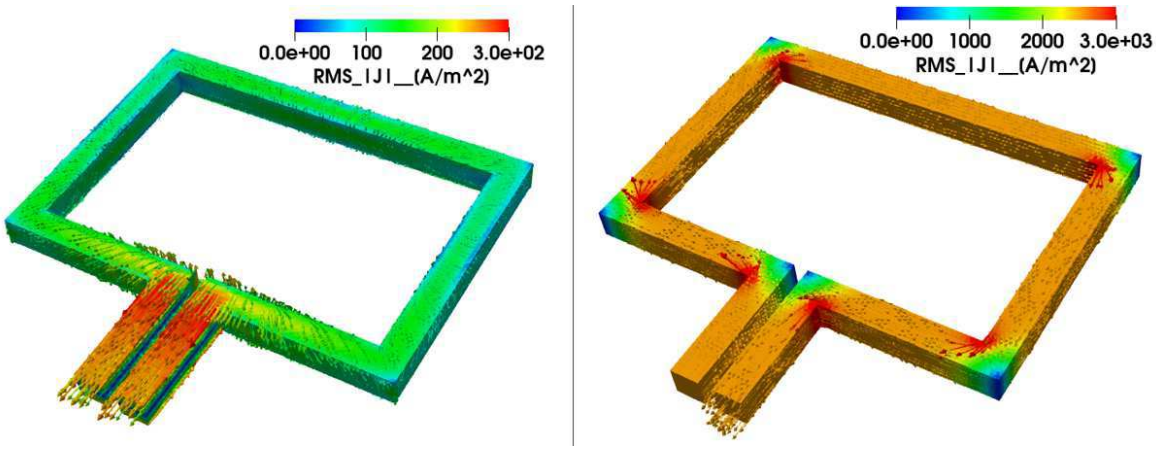

Figure 10: RMS strength of electric currents in a cross-section of the conducting loop for two choices of topological cycle bounding in Ω: choice τ_2 left, choice τ_2' right.

	No. of tets	J_2 for τ_2	J_2 for τ_2'
coarse mesh	298777	1.0034	$8.1 \cdot 10^{-6}$
medium mesh	347391	1.0023	$5.3 \cdot 10^{-6}$
fine mesh	599105	0.9999	$6.9 \cdot 10^{-6}$

Table 1: Currents J_2 for different choices of the topological cycles bounding w.r.t. Ω, see Fig. 9, and computed on tetrahedral meshes with different resolutions. The large fluctuations of the minute values of J_2 are due to discretization errors.

The simulation results compiled in Table 1 strikingly highlights that the choice of topological cycles with respect to connector cycles is crucial. We offer the following interpretation of the data of Table 1: The choice τ_2 does not intersect the straight connector cycle between Γ_E^1 and Γ_E^2, directs the electromotive force $\dot{B}_1^T$ along the conducting part of the split loop and, hence, engenders a strong current. Conversely, choosing τ_2' forces the connector cycle γ_2^E to wind around the tunnel and confines the electromotive force to the air gap, where it cannot cause a significant current.

References

[1] A. Alonso Rodriguez and A. Valli. “Voltage and current excitation for time-harmonic eddy current problems”. In: *SIAM J. Appl. Math.* 68 (2008), pp. 1477–1494.

[2] A. Bossavit. “Most general “non-local” boundary conditions for the Maxwell equations in a bounded region”. In: *COMPEL* 19.2 (2000), pp. 239–245.

[3] A. Buffa and R. Hiptmair. “Galerkin Boundary Element Methods for Electromagnetic Scattering”. In: *Topics in Computational Wave Propagation. Direct and inverse Problems*. Ed. by M. Ainsworth et al. Vol. 31. Lecture Notes in Computational Science and Engineering. Berlin: Springer, 2003, pp. 83–124.

[4] G. Ciuprina et al. “MEEC Models for RFIC Design Based on Coupled Electric and Magnetic Circuits”. In: *IEEE Transactions on Computer-Aided Design of Integrated Circuits and Systems* 34.3 (Mar. 2015), pp. 395–408.

[5] Gabriela Ciuprina et al. “Parameterized Model Order Reduction”. In: Jan. 2015, pp. 267–359.

[6] Ruben Dłotko Pawełand Specogna and Francesco Trevisan. "Automatic generation of cuts on large-sized meshes for the T-Ω geometric eddy-current formulation". In: *Comput. Methods Appl. Mech. Engrg.* 198.47-48 (2009), pp. 3765–3781.

[7] Harley Flanders. *Differential forms with applications to the physical sciences*. Academic Press, New York-London, 1963, pp. xiii+203.

[8] P.W. Gross and P.R. Kotiuga. *Electromagnetic Theory and Computation: A Topological Approach*. Vol. 48. Mathematical Sciences Research Institute Publications. Cambridge, UK: Cambridge University Press, 2004.

[9] R. Hiptmair. "Finite elements in computational electromagnetism". In: *Acta Numerica* 11 (2002), pp. 237–339.

[10] R. Hiptmair and J. Ostrowski. "Generators of $H_1(\Gamma_h, \mathbb{Z})$ for Triangulated Surfaces: Construction and Classification". In: *SIAM J. Computing* 31.5 (2002), pp. 1405–1423.

[11] R. Hiptmair and O. Sterz. "Current and voltage excitations for the eddy current model". In: *Int. J. Numer. Model* 18.1 (2005), pp. 1–21.

[12] Ralf Hiptmair, Peter Kotiuga, and Sébastien Tordeux. "Self-adjoint curl operators". In: *Annali di Matematica Pura ed Applicata* 191 (3 2012). 10.1007/s10231-011-0189-y, pp. 431–457.

[13] Daniel Ioan et al. "Models for integrated components coupled with their EM environment". In: *COMPEL: Int J for Computation and Maths. in Electrical and Electronic Eng.* 27.4 (2008), pp. 820–829.

[14] P.R. Kotiuga. "On making cuts for magnetic scalar potentials in multiply connected regions". In: *J. Appl. Phys.* 61.8 (1987), pp. 3916–3918.

[15] P.R. Kotiuga. "Topological duality in three-dimensional eddy-current problems and its role in computer-aided problem formulation". In: *J. Appl. Phys.* 9 (May 1990), pp. 4717–4719.

[16] P Monk. *Finite Element Methods for Maxwell's Equations*. Oxford, UK: Clarendon Press, 2003.

[17] S. Suuriniemi, J. Kangas, and L. Kettunen. "Driving a coupled field-circuit problem". In: *COMPEL* 26.3 (2007), pp. 899–909.

[18] S. Suuriniemi et al. "State variables for coupled circuit-field problems". In: *IEEE Transactions on Magnetics* 40.2 (Mar. 2004), pp. 949–952.